General Disclaimer

One or more of the Following Statements may affect this Document

- This document has been reproduced from the best copy furnished by the organizational source. It is being released in the interest of making available as much information as possible.

- This document may contain data, which exceeds the sheet parameters. It was furnished in this condition by the organizational source and is the best copy available.

- This document may contain tone-on-tone or color graphs, charts and/or pictures, which have been reproduced in black and white.

- This document is paginated as submitted by the original source.

- Portions of this document are not fully legible due to the historical nature of some of the material. However, it is the best reproduction available from the original submission.

Final Report

A STUDY OF ATMOSPHERIC EFFECTS ON PATTERN RECOGNITION DEVICES

F. THOMSON and F. SADOWSKI
Infrared and Optics Division

JULY 1975

Prepared for

NATIONAL AERONAUTICS AND SPACE ADMINISTRATION

Goddard Space Flight Center
Greenbelt, Maryland 20771
Contract No. NAS5-21783, Task III

1137A

ENVIRONMENTAL
RESEARCH INSTITUTE OF MICHIGAN
FORMERLY WILLOW RUN LABORATORIES. THE UNIVERSITY OF MICHIGAN
BOX 618 • ANN ARBOR • MICHIGAN 48107

TECHNICAL REPORT STANDARD TITLE PAGE

1. Report No.	2. Government Accession No.	3. Recipient's Catalog No.
NASA CR-ERIM 193300-62-F		

4. Title and Subtitle	5. Report Date
STUDY OF ATMOSPHERIC EFFECTS ON PATTERN RECOGNITION DEVICES	6. Performing Organization Code

7. Author(s)	8. Performing Organization Report No.
F. J. Thomson, F. G. Sadowski	193300-62-F

9. Performing Organization Name and Address	10. Work Unit No.
Environmental Research Institute of Michigan Infrared and Optics Division P.O. Box 618 Ann Arbor, Michigan 48107 (313) 994-1200	Task III
	11. Contract or Grant No. NAS5-21783
	13. Type of Report and Period Covered Final Report
12. Sponsoring Agency Name and Address National Aeronautics and Space Administration Goddard Space Flight Center Greenbelt Road Greenbelt, Maryland 20771	14. Sponsoring Agency Code

15. Supplementary Notes

Mr. Edmund F. Szajna (Code 430) monitored this work.

16. Abstract

This report describes a cooperative research project whose purpose is to demonstrate the types of terrain classes that can be mapped by applying computer-implemented pattern recognition to ERTS data in digital tape format. Results are also reported of a study to determine the effects on pattern recognition devices of changes in atmospheric effects caused by terrain elevation and atmospheric state changes within ERTS data.

17. Key Words	18. Distribution Statement
Atmospheric effects Pattern recognition devices EPTS-1 Scientific satellites	Initial distribution is listed at the end of this document.

19. Security Classif. (of this report)	20. Security Classif. (of this page)	21. No. of Pages	22. Price
UNCLASSIFIED	UNCLASSIFIED	66	

PREFACE

This report is submitted in fulfillment of National Aeronautics and Space Administration Contract No. NAS5-21783, Task III. Mr. Edmund F. Szajna was Technical Monitor for the project.

The purpose of our research was to demonstrate the use of computer-implemented pattern-recognition techniques in the preparation of terrain feature maps, and to determine the effects of changes in atmospheric paths over the test site on the performance of the pattern recognition classifier.

Work was done in cooperation with Dr. Harry Smedes of USGS/Denver, assisted by Mr. Jon Ranson of Colorado State University, and with Mr. Roland Hulstrom of Martin-Marietta Corporation in Denver. ERIM personnel who contributed to the success of the project included Dr. Robert Turner, who advised us on atmospheric models; Mr. Tom Austin and Mr. Dan Rice, who handled the computer processing; and Ms. Debbie Compton, who provided valuable secretarial support.

CONTENTS

FIGURES

TABLES

A STUDY OF ATMOSPHERIC EFFECTS ON PATTERN RECOGNITION DEVICES

1
INTRODUCTION

This is the final report on Task III of Contract NAS5-21783. The work was performed in cooperation with Dr. Harry Smedes of the U.S. Geological Survey (USGS), Denver, Colorado and Mr. Roland Hulstrom of the Martin-Marietta Corporation of Denver. Dr. Smedes was assisted by Mr. Jon Ranson, a Colorado State University graduate student. Work at ERIM was performed by Messrs. Frank Sadowski and Tom Austin under the direction of Fred Thomson, the Principal Investigator.

The project had two distinct phases. In Phase I, computer-implemented pattern-recognition techniques were used to prepare terrain feature maps from ERTS data collected over the Cripple Creek, Colorado test site on 20 August 1972. Because the base elevation in the test site ranges from 5000 to 14,000 ft MSL, we felt that the variation of atmospheric properties over the area would influence recognition. Hence, in Phase II, we wanted to determine the effects of the differences in atmospheric paths in various portions of the test site on the performance of the pattern recognition classifier. As an added effort, and as a preliminary step to working with the Colorado data, an agricultural scene near Sacramento, California was classified. Results of this latter work are presented in the Appendix.

1.1 COOPERATIVE ARRANGEMENTS

As briefly mentioned in the introduction, this work was a cooperative effort between Dr. Harry Smedes of USGS/Denver and Jon Ranson, a Colorado State University graduate student, and Roland Hulstrom of Martin-Marietta Corporation in Denver. Dr. Smedes established the geographic area in which the work was done, assisted in the definition of training sets and of terrain categories to be mapped, and assisted Jon Ranson in the assessment of map accuracy. ERIM provided data processing expertise and assisted in defining the terrain classes to be mapped.

Mr. Hulstrom made on-site radiometric measurements in the Cripple Creek test site for the ERTS overpasses of 16 February and 21 June 1973. These radiometric measurements of solar irradiance, atmospheric optical depth, and the reflectance and radiance of several large scene classes allowed us to investigate the variations of atmospheric state within the test site more completely.

Without the aid and assistance of these gentlemen, the project could not have been completed.

1.2 SUMMARY OF RESULTS

As a result of the investigation of atmospheric effects and of pattern recognition mapping of terrain classes in the Cripple Creek test site, the following results were obtained:

1) A thirteen-category recognition map was prepared, showing forest, water, grassland and exposed rock types. Preliminary assessment of classification accuracies showed that water, forest, meadow and Niobrara Shale were the most accurately mapped classes—70.6, 87.4, 73.7 and 85.7 percent correctly, respectively.

2) We attempted to discriminate sparse forest cover over different substrates, but the results were unsatisfactory. As a result, an intermediate forest class was created in the eleven-category map.

3) Investigations were made of the changes in accuracy of recognition caused by varying atmospheric effects with base elevation. The accuracy of water, forest, granodiorite and snow recognition were assessed. As base elevation varied from 7000 to 13,000 ft, with an atmospheric visibility of 48 km, no changes in water and forest recognition were observed (using the signatures for the thirteen-category map).

4) Granodiorite recognition accuracy decreased monotonically as base elevation increased, even though the training set location was at 10,000 ft elevation. This occurred because the covariance matrix size increased as base elevation increased (because of increases in irradiance and transmission with altitude), but mean values of the signature showed little change with elevation (path radiance changes offset the effects of irradiance and transmission). Since the volcanics signature closely resembled the granodiorite signature, misclassification of granodiorite as volcanic increased as base elevation increased.

5) The variation of snow signatures with base elevation was assessed with 160 km visibility. A simple pattern recognition device, a single band MSS-5 slicing algorithm, was assumed. For snow varying in base elevation from 9400 to 8420 ft, recognition decreases from 99% at the 9400-ft training set elevation to 88% at 8420 ft. The predicted degradation may not occur in practice with ERTS data because snow signals were clipped in ERTS band MSS-5.

6) Clipping of snow signals on 16 February 1973 Cripple Creek data occurs in bands MSS-4, -5, and -6. Calculations of expected radiance at the ERTS sensor from snow reflectance measured at the site and from Turner model calculations of irradiance, transmission and path radiance, reveal that snow signals should not be clipped, assuming that calculations and ERTS calibration constants were correct.

2
THEORETICAL DISCUSSION OF ATMOSPHERIC EFFECTS

In this section, the theory describing the effects of change in atmospheric properties is presented. First, the problem is formulated. Next, the variations of atmospheric attenuation and path radiance and of solar irradiance with visibility and elevation changes are discussed. Last, the changes in the spectral signatures caused by changes in atmospheric state are related to changes in classifier performance.

2.1 FORMULATION OF THE PROBLEM

If an assumed Lambertian reflecting object is viewed from space through a hazy atmosphere, the atmosphere modifies the radiance from the object by attenuation and addition of a path radiance term. Thus:

$$L_o(\lambda) = \frac{E(\lambda)\tau(\lambda)\rho(\lambda)}{\pi} + L_p(\lambda) \qquad (1)$$

where $L_o(\lambda)$ = the radiance observed from an object by a spaceborne sensor

$E(\lambda)$ = the total irradiance at ground level

$\tau(\lambda)$ = the atmospheric transmission from the object to the sensor along the sensor's line of sight

$\rho(\lambda)$ = the assumed Lambertian reflectance of the object

$L_p(\lambda)$ = the atmospheric path radiance along the sensor's line of sight

Generally, the total irradiance term is composed of a "specular" term which is attenuated sunlight, and a "diffuse" term which arises from atmospheric scattering. The attenuation of sunlight is generally different from τ because the path of the sunlight through the atmosphere is not the same as the sensor's line of sight (see Figure 1). The diffuse irradiance is caused by scattering and is generally larger in the blue spectral region than in the red because of the Rayleigh scattering.

Attenuation of radiance from the target is caused by scattering in the atmosphere or absorption by gases. Except for some absorption by ozone near 0.7 μm and water vapor near 0.92 μm, most of the attenuation of radiance in the ERTS bands is caused by scattering.

Path radiance is also caused by scattering in the atmosphere and consists of two terms. The spectrum of the first term often resembles that of the background in which the target is embedded. In addition to this background related term is the normal Rayleigh spectrum, with a larger contribution to path radiance in the blue region than in the red.

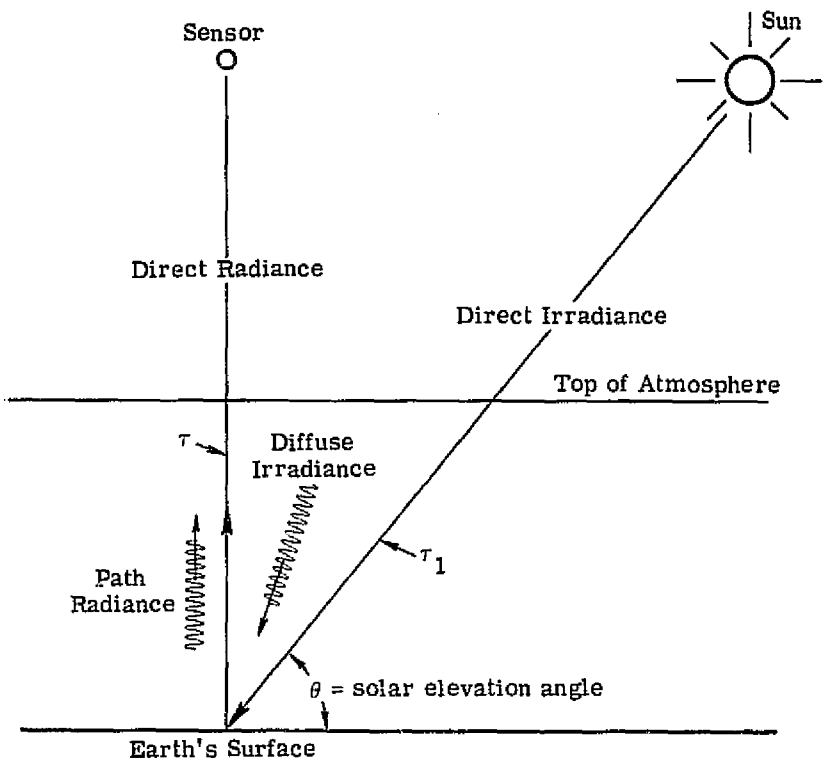

FIGURE 1. SIMPLIFIED DRAWING OF SOURCES OF ATTENUATION, IRRADIANCE, AND RADIANCE WHEN VIEWING THE EARTH

Typical supervised pattern classification algorithms require training before the algorithms can classify data. The training consists of entering the statistical descriptions (means and covariance matrix) of the multispectral radiance signatures of all classes to be recognized. The classifier then decides, on the basis of the radiance signature of an unknown point, to what class to assign that point. The class assigned is the one whose signature most closely resembles the signature of the unknown point. Since the assignment of classes is based on comparison, it follows that any effects which vary the radiance signature of one class from the training set location to the area being processed may affect the classification assigned to points within that area.

2.2 CHANGES IN ATMOSPHERIC EFFECTS CAUSED BY CHANGES IN ELEVATION

As the base elevation of the terrain changes, the optical properties of both the atmospheric paths traversed by the solar energy and those through which the sensor views the reflected energy from the terrain are changed. Qualitatively, as the base elevation increases, the total irradiance at ground level increases slightly. The direct irradiance (attenuated radiation from the sun) increases with increasing elevation because of lower attenuation in the atmospheric path from ground to sun. At the same time, and under normal atmospheric aerosol profiles where the aerosol concentration decreases smoothly with elevation, the diffuse irradiance (skylight) decreases because of reduced scattering. The reduced scattering is a consequence of both the reduced path aerosol concentration and the reduced path molecular concentration, affecting Mie and Rayleigh scattering respectively.

The atmospheric transmission from ground to sensor increases as the base elevation increases, for the same reason that the transmission from ground to sun increases. Additionally, the attenuation by water vapor at 0.92 μm decreases as base elevation increases. Ozone absorption at 0.7 μm does not change because the ozone layer is in the stratosphere. The path radiance in the ground-to-sensor path decreases as the base elevation increases, because of reduced scattering in the path.

What happens to the observed radiance from terrain objects as the base elevation varies depends on the refelectance of the object. For very low reflectance objects, most of the observed radiance is path radiance, hence the radiance of the object will decrease with increasing base elevation. Conversely, for very high reflectance objects, most of the observed radiance is reflected sunlight and skylight; thus the observed radiance for these objects will increase as base elevation increases. For intermediate values of object reflectance, observed radiance will either increase or decrease.

2.3 CHANGES IN CLASSIFIER PERFORMANCE CAUSED BY CHANGING ATMOSPHERIC EFFECTS

Regardless of the cause (either changing base elevation, changing atmospheric state, or change in background albedo), any change in atmospheric effects between the training set location and the location of the data being processed will affect the performance of a pattern recognition classifier. This is because the decision regarding the classification of any point is made by comparing the radiance signature of the point with the training set radiance signature stored in the computer.

If the training set signatures represent unbiased estimates of the signature statistics of each class, then the effect of altering the signatures of points to be classified by changing atmospheric effects will be to decrease the recognition accuracy for all classes. Misclassifications may increase or points may be assigned to a null category. (Assignment to the null category is made when the signature of a point does not closely resemble any of the training set signatures.) The amount of degradation in performance can be estimated once the training set signatures and the magnitude of changes in atmospheric effects are known. In general, the effect on recognition accuracy will be different for each class. Further, the degradation in accuracy will be greater (for a change in atmospheric effects of given size) if there are many similar classes rather than a few dissimilar classes being recognized. The work of Pitts and Potter [1, 2] supports these general remarks, although their results deal with horizontal variations and day-to-day variations in atmospheric state.

If changes in atmospheric state are extreme, the signatures of terrain classes will be drastically altered. If atmospheric attenuation increases, for example, the signature means and covariance matrix terms will be reduced. Because some part of the covariance terms is caused by sensor noise, which varies with observed radiance (in bands MSS-4, -5 and -6), the variation of covariance terms with changing atmospheric attenuation is different from the variation of signature mean values.

3
PRACTICAL INVESTIGATIONS OF ATMOSPHERIC EFFECTS IN THE CRIPPLE CREEK TEST SITE

In an effort to understand how changes in base elevation affected the signatures of common scene materials in the Cripple Creek site, atmospheric visibility measurements (for 20 August 1972) and on-site measured atmospheric properties (for 16 February 1973 and 21 June 1973) were used in an atmospheric model developed by R. Turner [3]. The Turner model computed values for the downwelling irradiance (both "specular" and "diffuse"), path transmission to the satellite, and path radiance as a function of elevation for wavelengths near the centers of the four ERTS bands. Then the changes of water, forest and rock signatures were assessed for 20 August 1972 data and changes of snow signatures were assessed for the 16 February data. The change in probability of misclassification for selected signature pairs was computed, assuming training sets at a low base elevation and data being classified at both low and high elevations.

Succeeding sub-sections present the analysis of each data set. The effect of signature changes on pattern recognition accuracy is summarized in a fourth sub-section.

3.1 ANALYSIS OF THE 20 AUGUST 1972 DATA SET (FRAME 1028-17135)

A great deal of analysis and pattern recognition processing was accomplished on the 20 August data set. The details of the pattern recognition processing and the preparation of a classification map for the Cripple Creek area will be presented in Section 4. This section discusses the calculation of atmospheric effects for various base elevations within the test site, and the resultant effects on several of the signatures used for preparing the recognition map.

3.1.1 ATMOSPHERIC MODEL CALCULATIONS

Because there were no on-site atmospheric measurements made during the 20 August 1972 overpass of the Cripple Creek site, atmospheric visibility conditions reported at Colorado Springs, on the eastern side of the test site, were used. At the 1713 GMT overpass of the ERTS satellite, Colorado Springs reported 30 mile (48 km) visibility. (Weather records summarizing the visibility and other meteorological data were obtained from the National Weather Records Center, Asheville, N.C.) Model calculations were made with a radiative transfer model developed by Dr. Robert Turner of ERIM [3]. The 48 km visibility reported at Salida, Colorado and 160 km visibility reported at Colorado Springs, Colorado were used to define the atmospheric state. The Turner model calculates the atmospheric optical thickness at each wavelength by reference to the Eltermann standard atmosphere. Calculations

were made at 7000, 9000, 11,000 and 13,000 ft elevation. A variety of background albedos, ranging from 2 to 64% were used. Wavelengths of 0.55, 0.65, 0.75, 0.85 and 0.95 μm were assumed. These wavelengths represented the center of each of the first three ERTS bands. Because of the large bandwidth and variation of sensor response over the bandwidth, two wavelengths were used for band MSS-7.

The Turner model calculates "specular" (solar) and "diffuse" irradiance, and path transmission and radiance in the ground-to-satellite path. These calculations are tabulated in Tables 1 through 3 for a green vegetation background and 48 km visibility. In looking at the data from Tables 1-3, the qualitative comments in Section 2 about the behavior of the irradiance, transmission and path radiance terms are confirmed. Further, note that the path radiance for the green band (0.55 μm) for a typical green vegetation background (about 0.16 albedo) is substantial. Even with the relatively high visibility and the high elevations of terrain, the path radiance in the green band at 7000 ft represents 12 counts on the digital tape, assuming the radiance scale factor as given in the ERTS Data User's Handbook [4] is correct.

3.1.2 EFFECTS OF ELEVATION VARIATIONS ON WATER, FOREST AND BARE ROCK RECOGNITION

In an effort to understand how base elevation variations affected the ability to recognize terrain features in the Cripple Creek test site, a simulation study was performed. Signatures for water, conifer forest and granodiorite were varied to simulate effects of base elevation. Then samples extracted from these signatures were classified, using the same training sets as for the recognition map to be discussed in Section 4. In this section the results of the simulation study are presented and discussed.

3.1.2.1 Simulation Procedure

Water, forest and exposed granodiorite were selected for study. Water is the darkest material in the scene at all wavelengths, so analysis of water recognition as a function of base elevation should reveal impacts of path radiance. Granodiorite is nearly the brightest material in the scene, so analysis of granodiorite recognition as a function of base elevation should reveal impacts of irradiance and path transmission variations. Finally, forest has nearly the same reflectance in all bands as the assumed green background, hence an analysis of forest recognition accuracy should reveal what happens to materials which closely resemble the background.

From an analysis of the locations of the areas selected for training sets, we found that forest training areas were at 7000 ft, water areas at 9000 ft, and exposed granodiorite areas at 10,000 ft. Using values for irradiance, path transmission and path radiance calculated with the Turner model, signatures were transformed to simulate those gathered from other base elevations. The transformation equations for mean and covariance information were:

TABLE 1. COMPUTED IRRADIANCE VERSUS ELEVATION FOR CRIPPLE CREEK TEST SITE, 20 AUGUST 1972

(a) Specular (Solar) Irradiance Versus Elevation

	Elevation (ft)			
Wavelength (μm)	7000	9000	11,000	13,000
0.55	105.93	106.67	107.35	108.01
0.65	99.66	100.01	100.33	100.64
0.75	83.94	84.10	84.25	84.40
0.85	68.53	68.62	69.70	68.77
0.95	58.50	58.54	58.58	58.64

(b) Diffuse (Sky) Irradiance Versus Elevation

	Elevation (ft)			
Wavelength (μm)	7000	9000	11,000	13,000
0.55	24.88	24.19	23.54	22.90
0.65	17.03	16.69	16.38	16.10
0.75	13.81	13.65	13.51	13.36
0.85	10.46	10.38	10.30	10.23
0.95	8.30	8.26	8.22	8.17

units are $mw/cm^2\ \mu$

TABLE 2. COMPUTED PATH TRANSMISSION VERSUS ELEVATION FOR CRIPPLE CREEK TEST SITE, 20 AUGUST 1972

	Elevation (ft)			
Wavelength (μm)	7000	9000	11,000	13,000
0.55	0.8107	0.8152	0.8194	0.8234
0.65	0.8583	0.8607	0.8629	0.8650
0.75	0.8791	0.8805	0.8817	0.8829
0.85	0.8922	0.8930	0.8939	0.8946
0.95	0.8990	0.8995	0.9001	0.9006

TABLE 3. COMPUTED PATH RADIANCE VERSUS ELEVATION FOR GREEN VEGETATION BACKGROUND FOR CRIPPLE CREEK TEST SITE, 20 AUGUST 1972

	Elevation (ft)			
Wavelength (μm)	7000	9000	11,000	13,000
0.55	2.319	2.297	2.276	2.257
0.65	1.008	1.002	0.996	0.991
0.75	1.194	1.184	1.175	1.166
0.85	1.058	1.045	1.037	1.031
0.95	0.797	0.793	0.789	0.785

units are mw/cm^2 sr μ

$$M_{hi} = M_{si} \times \frac{E_{hi}\tau_{hi}}{E_{si}\tau_{si}} + (L_{phi} - L_{psi}) \times \frac{I_{fsi}}{S_i} \quad (2)$$

$$V_{hij} = V_{sij}\left(\frac{E_{hi}\tau_{hi}E_{nj}\tau_{nj}}{E_{si}\tau_{si}E_{sj}\tau_{sj}}\right) \quad (3)$$

where M_{hi} = mean at altitude h in band i (in units of digital counts)

M_{si} = mean at standard altitude in band i (in units of digital counts)

V_{hij} = covariance between bands i and j at altitude h

V_{sij} = covariance between bands i and j at standard altitude

E_{hi} = total irradiance at altitude h in band i

τ_{hi} = path transmission at altitude h in band i

E_{si} = total irradiance at standard altitude in band i

τ_{si} = path transmission at standard altitude in band i

L_{phi} = path radiance at altitude h in band i

L_{psi} = path radiance at standard altitude in band i

I_{fsi} = full scale digital tape integer level in band i

S_i = nominal full scale radiance in band i from ERTS Data User's Handbook

E_{nj} = total irradiance at altitude h in band j

τ_{hj} = path transmission at altitude h in band j

E_{sj} = total irradiance at standard altitude in band j

τ_{sj} = path transmission at standard altitude in band j

After all means and covariance matrices had been altered to provide simulated signatures at 7000, 9000, 11,000 and 13,000 ft for water, forest and granodiorite, 1000 samples were selected from each signature. In selecting the samples, the multivariate gaussian assumption was made. Then these samples were classified using the 21 training sets selected for the terrain mapping task. Tables showing how the points were classified (confusion matrices) were produced.

3.1.2.2 Analysis of Results

The classification accuracy as a function of the base elevation is given in Table 4.

Note that in Table 4 the accuracy of classification of water, expressed as a percentage, does not vary as we move up in elevation from 7000 to 13,000 ft. The signature of water does

change, but the decision region for water (that area of four dimensional hyperspace inside which data values are called water) is large enough to encompass all the variations caused by changes in elevation with 48 km atmospheric visibility.

TABLE 4. CLASSIFICATION ACCURACY AS A FUNCTION OF BASE ELEVATION FOR THREE MATERIALS

Elevation (ft)	Water*	Forest**	Granodiorite***
7000	99.8%	99.4%	83.5%
9000	99.8	99.4	83.2
11,000	99.8	99.4	82.2
13,000	99.8	99.3	81.5

*0.2% misclassified as Cloud Shadow

**0.6-0.7% misclassified as Alpine Composite

***12.6-14.9% misclassified as Exposed Volcanics and 2.1-2.3% misclassifed as Dakota Sandstone Composite

Granodiorite recognition shows a different pattern. Because the reflectance of granodiorite is larger than either water or coniferous forest in all ERTS bands, we expect path transmission and irradiance effects to predominate. The results shown in Table 4 were somewhat unexpected because the recognition accuracy of granodiorite improves as the base elevation decreases. We might expect that the recognition accuracy would decrease as we got farther away, in either direction, from the 10,000 ft elevation training set location. The explanation for the observed variations in classification accuracy is as follows. As we move away from the 10,000 ft training set elevation the mean values of the granodiorite signatures are modified by the irradiance and transmission variations (multiplicative) and the path radiance (additive). The irradiance and transmission and path radiance variations are negatively correlated, so that an increase in one means a decrease in the other. The result of these variations, at 48 km visibility, is that the granodiorite signature means shift very little from 7000 to 13,000 ft. The change in means is 0.003σ, 0.0016σ, 0.0001σ, and 0.0013σ for MSS-4 through MSS-7 respectively. By contrast, the size of the signature (as measured by the product of the four eigenvalues) increases by 6% when going from 7000 to 13,000 ft. This means that the signature mean remains virtually unaltered, but that the size of the 1σ hyperellipse increases as we go from 7000 to 13,000 ft. The effec' of this is to increase the misclassification of granodiorite as the base elevation increases. As the recognition accuracy of granodiorite decreases monotonically with increasing base elevation, its misclassification as exposed volcanics and as Dakota sandstone composite monotonically increases.

3.1.2.3 Summary

In summary then, for the 48 km atmospheric visibility case and for the classes and classifier structure examined, the major atmospheric effect as base elevation is increased is to monotonically decrease the recognition accuracy of granodiorite. The recognition accuracy of low albedo targets, such as water and forest, is not affected because their associated decision regions are large.

3.2 ANALYSIS OF THE 16 FEBRUARY 1973 DATA SET (FRAME 1116-17135)

The 16 February data set over the Cripple Creek area was selected for analysis because the ground was covered with snow. Snow is a very high reflectance material (≈85%) in all four bands of the ERTS-MSS sensor. We felt that examination of the effects of atmosphere on snow signatures as a function of altitude would give us an understanding of the impact of changing irradiance and path transmission on the performance of pattern recognition devices.

3.2.1 MARTIN-MARIETTA MEASUREMENTS

Two test sites within the Cripple Creek Test Area were manned by Martin-Marietta personnel under the direction of Roland Hulstrom. The sites (see Figure 2) were Granite Hills

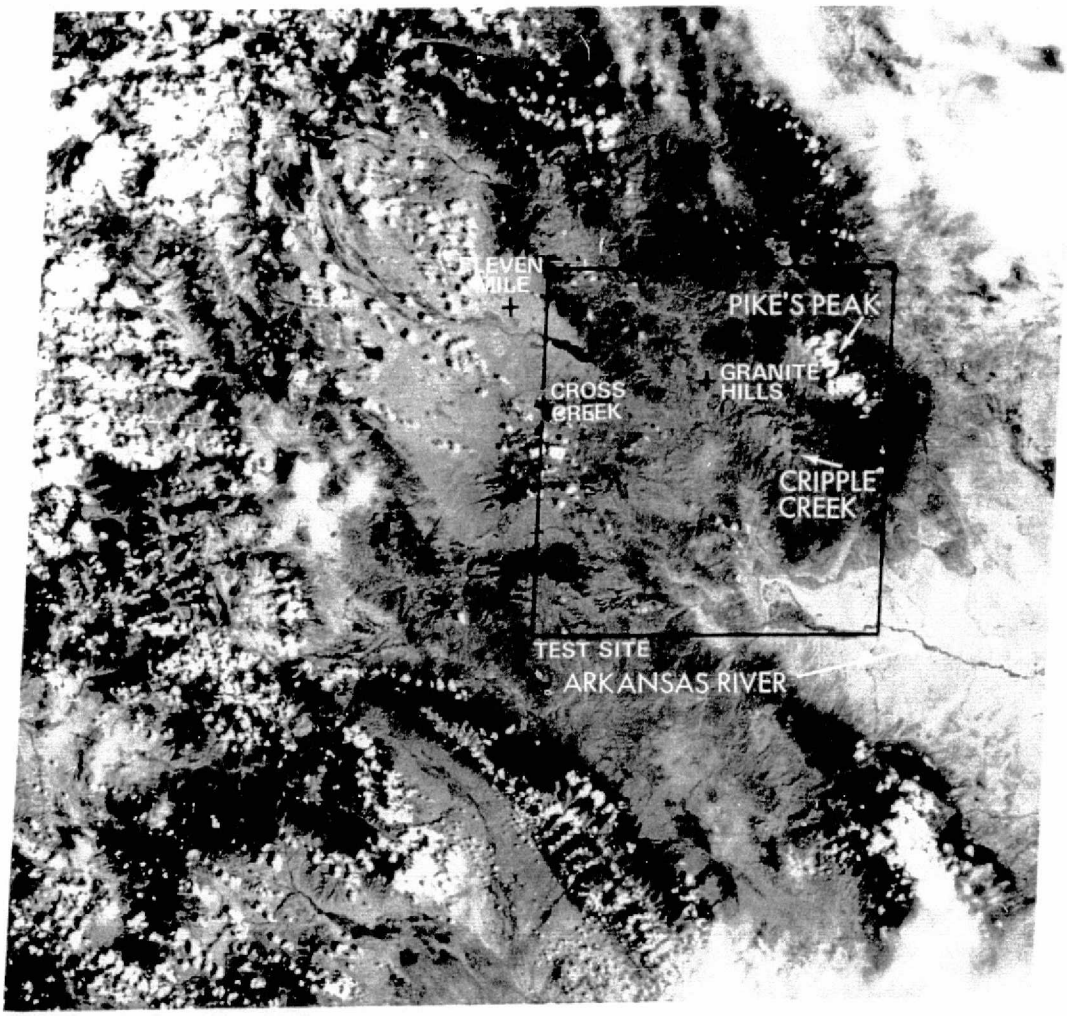

FIGURE 2. ERTS MSS-5 IMAGERY OF CRIPPLE CREEK TEST SITE, SHOWING TEST SITE BOUNDARY AND ATMOSPHERIC PROPERTY MEASUREMENT SITES

(elevation 8240 ft) and Eleven Mile Reservoir (elevation 9400 ft). At both sites the solar irradiance and optical thickness of the atmosphere were determined. At the Eleven Mile Reservoir site the reflectance and radiance of six different snow areas within a mile of the test site were measured.

Tables 5, 6, and 7 present the measurements made by Martin-Marietta as summarized in Reference [5]. Table 7 also presents the snow mean (ρ_{mean}) and standard deviation (ρ_{SD}) reflectances computed from the Martin-Marietta data. Since the Martin-Marietta data were measured with a Bendix RPMI, only band-averaged reflectance, irradiance, and atmospheric optical thickness values are presented. The Martin-Marietta measurements were made within a few minutes of the calculated ERTS overpass, so the conditions under which ERTS data were collected were faithfully recorded.

3.2.2 ATMOSPHERIC MODEL CALCULATIONS

The Martin-Marietta atmospheric optical thickness measurements were used in the Turner model to calculate the atmospheric transmission, path radiance and ground irradiance for a variety of background albedo conditions. Calculations for both the Granite Hills and Eleven Mile Reservoir sites were made. For purposes of these calculations, wavelengths at the centroid of the RPMI bands (calculated from nominal sensitivity curves supplied by Bendix) were used.

The Turner calculations are summarized in Tables 8 (Irradiance), 9 (Transmission), and 10 (Path Radiance). For irradiance and path radiance, only results of calculations at the background albedo of snow are presented. As expected, in each wavelength the direct (solar) irradiance and transmission are higher for the Eleven Mile Reservoir site than for the Granite Hills site, while diffuse irradiance and path radiances are lower for the Eleven Mile site than for Granite Hills. As explained in Section 2, this behavior is explained by the higher elevation, lower atmospheric optical depth and reduced scattering at the Eleven Mile Reservoir site.

3.2.3 COMPARISON OF MODEL CALCULATIONS AND HULSTROM MEASUREMENTS

In an effort to compare the model calculations with the Hulstrom measurements, values of total irradiance were compared. The comparison should reveal if the model has correctly partitioned the measured optical thickness between Rayleigh, ozone, and non-Rayleigh terms. Since each of these scattering and absorption processes has a different spectral behavior, any difference in curve shape between the measured and calculated results would be indicative of incorrect partition.

TABLE 5. ATMOSPHERIC OPTICAL DEPTH AT TWO SITES IN THE CRIPPLE CREEK TEST AREA ON 16 FEBRUARY 1973

	MSS Band			
Site	4	5	6	7
Granite Hills	0.179	0.137	0.109	0.069
Eleven Mile Reservoir	0.137	0.101	0.066	0.052

TABLE 6. SOLAR IRRADIANCE AT TWO SITES IN THE CRIPPLE CREEK TEST AREA ON 16 FEBRUARY 1973

	MSS Band			
Site	4	5	6	7
Granite Hills	65.8	56.8	47.9	76.4
Eleven Mile Reservoir	91.7	75.6	64.5	122.9

units are w/m^2

TABLE 7. REFLECTANCE OF SNOW FIELDS AT ELEVEN MILE RESERVOIR, 16 FEBRUARY 1973

	Samples							
MSS Band	1	2	3	4	5	6	ρ_{Mean}	ρ_{SD}
4	0.86	0.83	0.84	0.86	0.84	0.86	0.8483	0.0148
5	0.87	0.83	0.86	0.86	0.84	0.86	0.8533	0.0137
6	0.87	0.82	0.84	0.87	0.83	0.84	0.8450	0.0160
7	0.75	0.73	0.79	0.79	0.73	0.77	0.7600	0.0252

TABLE 8. TURNER MODEL CALCULATED IRRADIANCES FOR TWO SITES IN THE CRIPPLE CREEK TEST AREA, 16 FEBRUARY 1973

(a) Granite Hills Site

Wavelength (μm)	Solar Irradiance (mw/cm^2 μ)	Diffuse Irradiance (mw/cm^2 μ)*
0.56	63.1915	25.4348
0.68	57.7203	17.2330
0.76	51.7201	11.9841
0.91	40.6188	5.6845

(b) Eleven Mile Reservoir Site

Wavelength (μm)	Solar Irradiance (mw/cm^2 μ)	Diffuse Irradiance (mw/cm^2 μ)*
0.56	68.5606	20.1318
0.68	61.8992	13.0916
0.76	56.2235	7.5134
0.91	41.9819	4.3352

*only diffuse irradiance for a background albedo of 0.85 is shown, except for Band 7 (0.91 μm) where the background albedo is 0.75.

TABLE 9. TURNER MODEL CALCULATED PATH TRANSMISSION FOR TWO SITES IN THE CRIPPLE CREEK TEST AREA, 16 FEBRUARY 1973

(a) Granite Hills Site

Wavelength (μm)	Transmission
0.56	0.8361
0.68	0.8720
0.76	0.8967
0.91	0.9333

(b) Eleven Mile Reservoir Site

Wavelength (μm)	Transmission
0.56	0.8720
0.68	0.9039
0.76	0.9361
0.91	0.9493

TABLE 10. TURNER MODEL CALCULATED PATH RADIANCES FOR TWO SITES IN THE CRIPPLE CREEK TEST AREA, 16 FEBRUARY 1973

(a) Granite Hills Site

Wavelength (μm)	Background Albedo	Path Radiance (mw/cm^2 sr μ)
0.56	0.85	2.9892
0.68	0.85	1.7835
0.76	0.85	1.1841
0.91	0.76	0.4919

(b) Eleven Mile Reservoir Site

Wavelength (μm)	Background Albedo	Path Radiance (mw/cm^2 sr μ)
0.56	0.85	2.4670
0.68	0.85	1.3974
0.76	0.85	0.7846
0.91	0.76	0.3845

Figure 3 shows the results of the comparison of measured and calculated values for total irradiance, over each ERTS bandwidth, for the Eleven Mile Reservoir site. Agreement between the Hulstrom measured values and Turner calculated values are good, with the greatest discrepancy occurring in band MSS-7. This discrepancy may occur because of the use of an improper normalizing factor (0.3) to convert the Hulstrom RPMI band average irradiance to spectral irradiance. The value 0.3 was the nominal spectral bandwidth of the MSS-7 RPMI channel. If the equivalent bandwidth were effectively narrower, corresponding to a response skewed toward the visible end of the spectrum, the Hulstrom measurements would be larger and in closer agreement with the Turner measurements. In any case, the agreement between the model calculations and the measurements is good for the Eleven Mile Reservoir site.

For the Granite Hills site (Figure 4), the model calculations are consistently larger than the Hulstrom measurements by factors of 1.347, 1.3202, 1.331 and 1.819 for bands MSS-4, -5, -6 and -7 respectively. There is a relatively constant factor relating Turner model irradiances to Hulstrom irradiances in the first three bands, where we observed close agreement at the Eleven Mile Reservoir. The factor is larger for MSS-7, and this too is in agreement with the comparison at the Eleven Mile Reservoir Site where Turner's model calculated a higher irradiance than Hulstrom observed.

The Hulstrom report [5] states that both sites were manned, and measurements made, simultaneously. If this is so, we would expect that the solar irradiances at the two sites would be in the ratio of the difference of optical thicknesses times the secant of the solar zenith angle. Unfortunately, although it is possible to measure values of solar irradiance with the RPMI, these values were not reported, so we cannot check this hypothesis. The only factor that could account for the lower measured irradiance at Granite Hills is that measurements were actually made earlier than at Eleven Mile Reservoir. The Turner model calculations are viewed as representative of the actual conditions.

3.2.4 EFFECTS OF ATMOSPHERIC VARIATION ON SNOW SIGNATURES

Using the Turner model calculations for the two sites, we calculated the radiance of snow for each site. Then the radiance differences were compared to the radiance difference at each site caused by the normal variation of snow reflectance, as calculated from Hulstrom measurements at the Eleven Mile Reservoir site. A large variation between sites compared to within-site variation means that the change in signature mean caused by elevation variations is significant.

Tables 11 and 12 are snow radiance calculations for the Eleven Mile Reservoir site. The radiances calculated are those seen by the satellite, so the effects of atmospheric attenuation and path radiance are included. The snow radiances were computed by the formula:

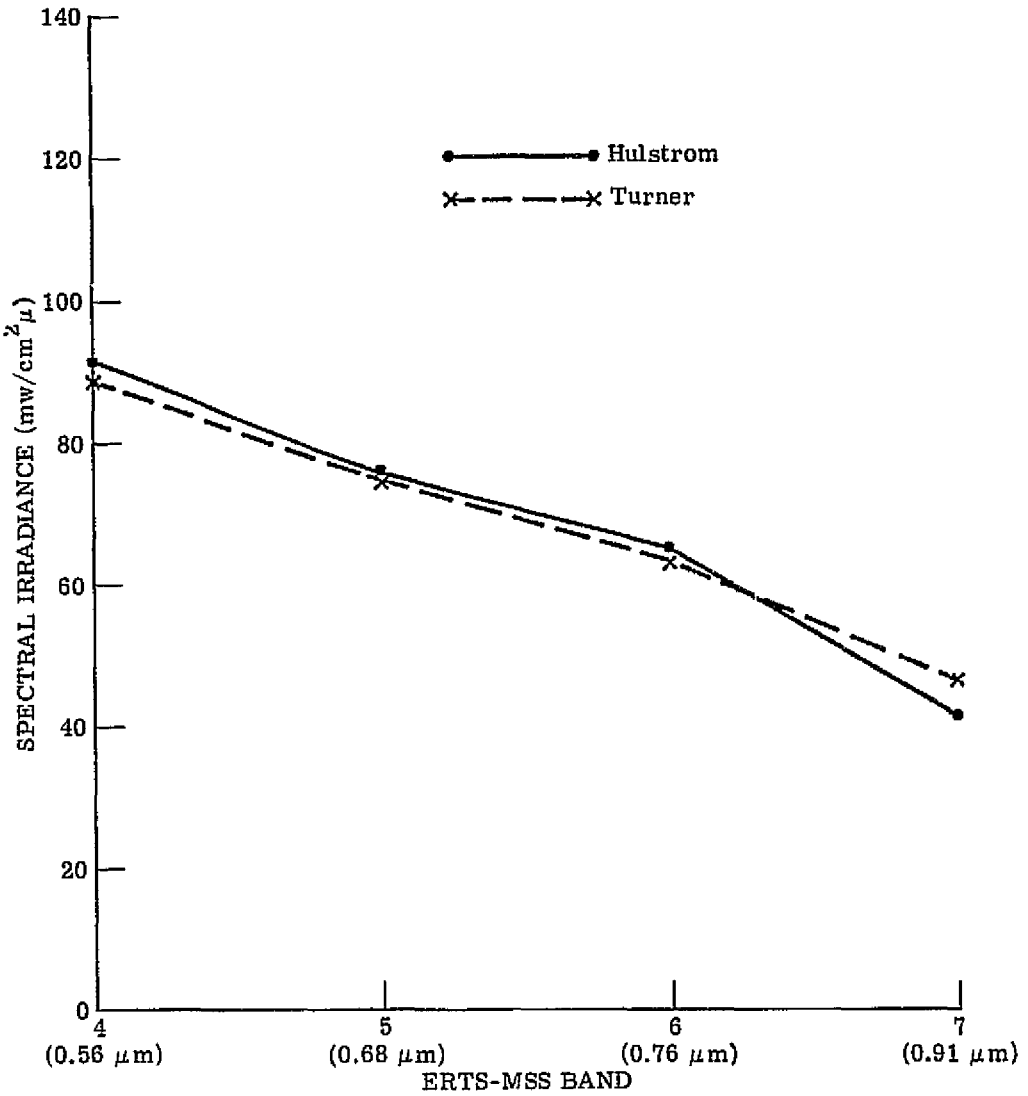

FIGURE 3. COMPARISON OF HULSTROM MEASURED AND TURNER MODEL TOTAL IRRADIANCE FOR ELEVEN MILE RESERVOIR SITE, 16 FEBRUARY 1973

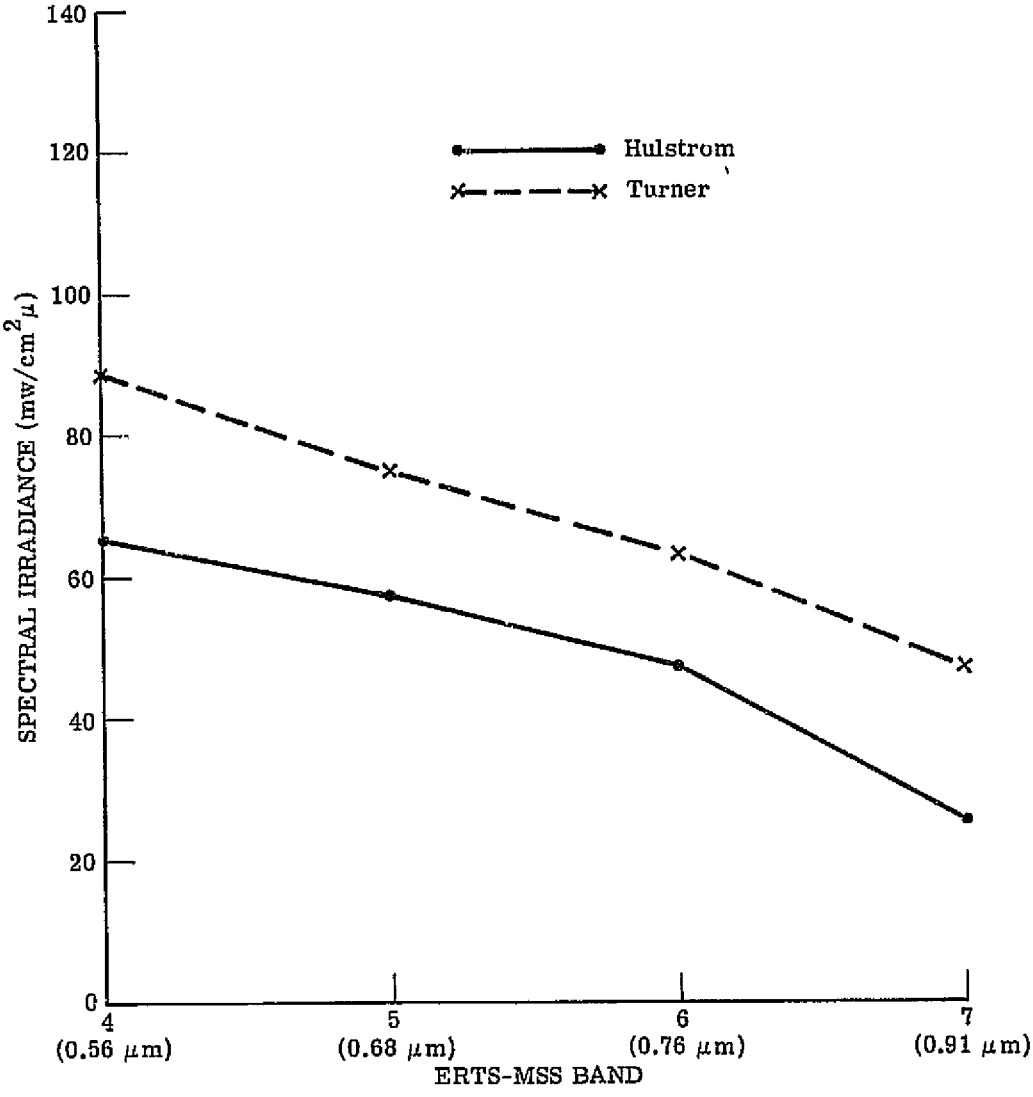

FIGURE 4. COMPARISON OF HULSTROM MEASURED AND TURNER MODEL TOTAL IRRADIANCE FOR GRANITE HILLS SITE, 16 FEBRUARY 1973

TABLE 11. CALCULATED SNOW RADIANCE (AS VIEWED BY ERTS) FOR ELEVEN MILE RESERVOIR SITE, 16 FEBRUARY 1973

Wavelength (μm)	MSS Band	Snow Spectral Radiance (mw/cm^2 sr μ)
0.56	4	23.350
0.68	5	19.808
0.76	6	16.833
0.91	7	11.021

TABLE 12. CALCULATED SNOW RADIANCE (AS VIEWED BY ERTS) FOR GRANITE HILLS SITE, 16 FEBRUARY 1973

Wavelength (μm)	MSS Band	Snow Spectral Radiance (mw/cm^2 sr μ)
0.56	4	22.998
0.68	5	19.036
0.76	6	16.549
0.91	7	10.946

$$L = \frac{\rho_{snow} E \tau}{\pi} + L_p \qquad (4)$$

where ρ_{snow} = snow reflectance

E = total spectral irradiance

τ = atmospheric transmission

L_p = atmosphere spectral path radiance

The path radiance and irradiance values used were for snow background.

Table 13 presents the radiances corresponding to one standard deviation of the snow reflectance signature at each site. A quick comparison of mean differences and the radiance corresponding to one standard deviation reveals that the shift in signature means is 0.987, 2.45, 0.955 and 0.214 standard deviations in bands MSS-4 through MSS-7 respectively. The χ^2 distance between the signatures is 3.423, which is significant at the 0.35 level for four degrees of freedom. Thus the probability is only 35% that a random sample of one snow signature would fall at the mean of the other snow signature. The varying effect of the atmosphere at 8420 and 9400 ft elevation has caused the snow signature to shift by a significant amount.

The impact of the variation in atmospheric effects on the performance of a pattern recognition device can be estimated as follows. Suppose, in this case, that the pattern recognition device is simply an MSS-5 level slicing device. The decision is made that a pixel of ERTS data represents snow if the digital value is between two levels which are set by analysis of a snow training set signature. Suppose the levels were set to recognize 99% of the snow at 8240 ft. Then the levels would be 2.51σ away from the snow mean signal at 8240 ft. These threshold limits would recognize 87.9% of the snow at 9400 ft. The reduction in accuracy is caused by the change in the mean value of the snow signature and the increase in the standard deviation of that signature at the higher elevation. The effects are noticable, even in the very clear atmospheric conditions we had for the 16 February 1973 data, but the acceptability of this performance is a decision for the user. We recommend careful study of this aspect of snow recognition by those engaged in the snow mapping Applications System Verification Test.

3.2.5 VERIFICATION OF SIGNATURES

In an attempt to verify the variation of snow signatures with base elevation, we selected snow signatures from the 16 February 1973 ERTS data and attempted an analysis of ERTS-MSS signal levels. We found that the snow signatures saturated the first three channels of the ERTS sensor. This was unexpected, as the calculations of snow radiance (Tables 10 and 11) showed that there should have been a sizable number of unsaturated data values in these three bands if the calibration constants given in the ERTS Data User's Handbook [4] were correct.

TABLE 13. RADIANCE DIFFERENCES CORRESPONDING TO ONE STANDARD DEVIATION FOR SNOW SIGNATURE

Wavelength (μm)	MSS Band	Eleven Mile Radiance (mw/cm^2 sr μ)	Granite Hills Radiance (mw/cm^2 sr μ)
0.56	4	0.3644	0.3490
0.68	5	0.2956	0.3350
0.76	6	0.3038	0.2910
0.91	7	0.3527	0.3466

units are mw/cm^2 sr μ

Because of this discrepancy, we can only conclude that our calculated snow radiances are too small or that the ERTS calibration constants are too large. This difficulty precluded further analysis of signatures and verification of the calculated variation caused by elevation differences.

3.3 ANALYSIS OF THE 21 JUNE 1973 DATA SET (FRAME 1208-17135)

The 21 June data set collected over the Cripple Creek test site offered an opportunity to examine the effects of elevation on vegetation, rock and water signatures and to further compare Hulstrom measurements of irradiance with Turner model calculations. A further comparison was made of Hulstrom's measurements of atmospheric optical depth with those computed from visibilities estimated by weather stations in the area.

3.3.1 MARTIN-MARIETTA MEASUREMENTS

For the 21 June overpass of the ERTS satellite, Granite Hills and Cross Creek stations were visited and measurements made (see Figure 2). On this trip, spectral solar and diffuse irradiances were measured from 0.5 - 1.1 μm in 0.25 μm intervals (0.5 - 0.75 μm) and 0.50 μm intervals (0.75 - 1.1 μm). Measurements were made with an ISCO spectro radiometer. A Bendix RPMI was used for atmospheric optical depth measurements [6]. Measurements of the spectral reflectance of basalt at Cross Creek and the Pikes Peak granite were made with the ISCO. Measurements of optical depth of the atmosphere were made near the time of ERTS overpass at the Granite Hills site and 1 1/2 hours after overpass at the Cross Creek site. Tables 14, 15, and 16 present atmospheric optical depth, spectral irradiance and reflectance data from the Martin-Marietta measurements. Values of the latter two parameters were obtained from graphs [6], and so may not be as accurate as the optical depth values.

3.3.2 ATMOSPHERIC MODEL CALCULATIONS

As with the 16 February 1973 data, the Martin-Marietta optical thickness measurements were used in the Turner model to calculate atmospheric transmission, path radiance, and ground irradiance. The same wavelengths at the centroids of the RPMI bands were used.

The Turner model calculations are summarized in Tables 17 (Irradiance), 18 (Transmission), and 19 (Path Radiance). For irradiance and path radiance, only results of calculations at the albedo of green vegetation are presented. The albedo of green vegetation is assumed to be 0.12, 0.08, 0.4, and 0.64 for bands MSS-4 through -7 respectively.

3.3.3 COMPARISON OF MODEL CALCULATIONS AND HULSTROM MEASUREMENTS

Only the Hulstrom measurements at the Granite Hills site may be directly compared with the model calculations since both were made for the time of ERTS overpass. The measurements

TABLE 14. ATMOSPHERIC OPTICAL DEPTH AT TWO SITES WITHIN THE CRIPPLE CREEK TEST AREA, 21 JUNE 1973

(a) Cross Creek - 1854 GMT

Wavelength (μm)	MSS Band	Atmospheric Optical Depth
0.56	4	0.159
0.68	5	0.122
0.76	6	0.078
0.91	7	0.058

(b) Granite Hills - 1730 GMT

Wavelength (μm)	MSS Band	Atmospheric Optical Depth
0.56	4	0.157
0.68	5	0.122
0.76	6	0.082
0.91	7	0.063

TABLE 15. SPECTRAL TOTAL AND DIFFUSE IRRADIANCES AT TWO SITES WITHIN THE CRIPPLE CREEK TEST AREA, 21 JUNE 1973

(a) Granite Hills: 1725-1728 GMT

Wavelength	Total Irradiance ($mw/cm^2\ \mu$)	Diffuse Irradiance ($mw/cm^2\ \mu$)
0.5	168.0	10.6
0.525	151.0	9.0
0.550	150.0	8.0
0.575	148.0	6.6
0.600	143.0	6.0
0.625	139.0	5.3
0.650	133.0	4.6
0.675	131.0	4.2
0.700	119.0	3.5
0.725	108.0	3.4
0.750	99.0	3.1
0.800	85.0	2.5
0.850	75.0	2.3
0.900	58.0	1.7
0.950	14.8	1.1
1.000	19.3	1.1
1.050	17.0	0.9
1.100	2.8	0.6

(b) Cross Creek Site

Wavelength	Total Irradiance ($mw/cm^2\ \mu$)	Diffuse Irradiance ($mw/cm^2\ \mu$)
0.500	175.0	11.8
0.525	155.0	8.9
0.550	144.0	6.7
0.575	134.0	6.8
0.600	132.0	4.6
0.625	127.0	3.6
0.650	120.0	3.4
0.675	113.0	2.9
0.700	102.0	2.6
0.725	-	2.5
0.750	97.0	2.5
0.800	89.0	-
0.850	64.0	-
0.900	50.0	-
0.950	35.2	-
1.000	35.2	-
1.050	26.1	-
1.100	15.9	-

TABLE 16. REFLECTANCES OF COMMON MATERIALS MEASURED WITH THE ISCO AND RPMI SPECTRORADIOMETERS CRIPPLE CREEK TEST SITE, 21 JUNE 1973

(a) ISCO Measurements

Wavelength	Pikes Peak Granite*	Basalt**
0.500	11	6
0.525	12	8
0.550	14	9
0.575	16	10
0.600	17	11
0.625	18	11
0.650	-	11
0.675	18	12
0.700	20	12
0.725	21	13
0.750	22	14
0.800	-	15
0.850	-	16
0.900	25	17
0.950	25	20
1.000	26	20
1.050	27	21
1.100	28	-

*measured at Granite Hills
**measured at Cross Creek

(b) RPMI Measurements

Material	MSS Band (Wavelength) 4 (0.56)	5 (0.68)	6 (0.76)	7 (0.91)
Pikes Peak Granite	14.2	19.0	21.0	21.2
Cripple Creek Granite	14.5	15.9	22.2	25.3
39 Mile Basalt	10.0	13.8	16.5	18.0
Carlisle Shale	45.0	50.0	53.8	56.0
Dakota Formation	32.0	40.0	37.9	51.0

TABLE 17. CALCULATED TOTAL AND DIFFUSE IRRADIANCE FOR GREEN VEGETATION BACKGROUND: CRIPPLE CREEK TEST SITE, 21 JUNE 1973

(a) Granite Hills Site

Wavelength (μm)	MSS Band	Total Irradiance (mw/cm^2 μ)	Diffuse Irradiance (mw/cm^2 μ)
0.56	4	121.2930	18.9134
0.68	5	106.2443	13.5317
0.76	6	94.3410	8.7524
0.91	7	70.0462	5.2528

(b) Cross Creek Site

Wavelength (μm)	MSS Band	Total Irradiance (mw/cm^2 μ)	Diffuse Irradiance (mw/cm^2 μ)
0.56	4	121.0186	19.3437
0.68	5	106.2443	13.6023
0.76	6	95.6319	7.4810
0.91	7	70.4440	4.8511

TABLE 18. CALCULATED ATMOSPHERIC TRANSMISSION FOR CRIPPLE CREEK SITE, 21 JUNE 1973

(a) Granite Hills Site

Wavelength (μm)	MSS Band	Transmission
0.56	4	0.8547
0.68	5	0.8851
0.76	6	0.9213
0.91	7	0.9389

(b) Cross Creek Site

Wavelength (μm)	MSS Band	Transmission
0.56	4	0.8530
0.68	5	0.8851
0.76	6	0.9250
0.91	7	0.9436

TABLE 19. CALCULATED PATH RADIANCE FOR A GREEN VEGETATION BACKGROUND: CRIPPLE CREEK TEST SITE, 21 JUNE 1973

(a) Granite Hills Site

Wavelength (μm)	MSS Band	Path Radiance (mw/cm^2 sr μ)
0.56	4	1.8797
0.68	5	0.8913
0.76	6	0.9067
0.91	7	0.6357

(b) Cross Creek Site

Wavelength (μm)	MSS Band	Path Radiance (mw/cm^2 sr μ)
0.56	4	1.8553
0.68	5	0.8760
0.76	6	0.8646
0.91	7	0.5888

were made 1 1/2 hours later than the ERTS overpass at the Cross Creek site. Because there were spectral measurements of both total and diffuse spectral irradiance, these quantities can be compared.

Figure 5 shows the total spectral irradiance from Hulstrom measurements and the single-wavelength Turner model calculations. Good qualitative agreement between the measurements and calculations is shown although there is a tendency for the Turner calculations to overestimate irradiance at the longer wavelengths and to underestimate it at shorter wavelengths. The differences between the two measurements are -2.8, -6.25, 14.4 and 33% for 0.56, 0.68, 0.76 and 0.91 μm, assuming that the Hulstrom measurements are correct.

Figure 6 compares Turner model calculated diffuse irradiance (divided by 2) to the Hulstrom measured values. The similar curves seem to indicate that the variation with wavelength for the calculated results is the same as for the measured results. This, in turn would indicate a proper partition of the total optical depth between Rayleigh and aerosol terms. The Turner calculated values are over a factor of 2 greater than the Hulstrom measured values. The Hulstrom report [6] contains the notation that diffuse spectral irradiances measurements were made with a 6 ft fiber optics probe on the ISCO. Such a probe restricts the field of view of the instrument to less than a hemisphere. Consequently, less diffuse irradiance is measured because the solid angle viewed is smaller. The fiber optics bundle was also used to measure total irradiance; but for that measurement the effects are less severe, because of the dominating influence of the direct solar irradiance term at these low atmospheric optical depth conditions.

3.3.4 COMPARISON OF HULSTROM MEASUREMENTS WITH WEATHER DATA VISIBILITIES

In an effort to assess the practicality of using visibility data reported by the National Weather Service as a model input, we compared the Hulstrom measurements of optical depth to those which we would have obtained from visibility estimates from surrounding stations. In so doing, we were aware of two problems which would compromise the comparison. First, the surrounding weather stations were at different base elevations from the measurement site. Even in the presence of a horizontally uniform atmosphere, we needed some way of extrapolating measurements made at weather station elevations to the test site elevations. Second, we were aware that weather observers' estimates of visibility depend on the location of certain landmarks; when visibility is good, estimates can be inaccurate because of a lack of landmarks at long distances (~100 km).

The procedure was to convert weather station visibility estimates from Colorado Springs and Salida to optical depths at 0.56 μm. Then, the equivalent optical depth at Granite Hills

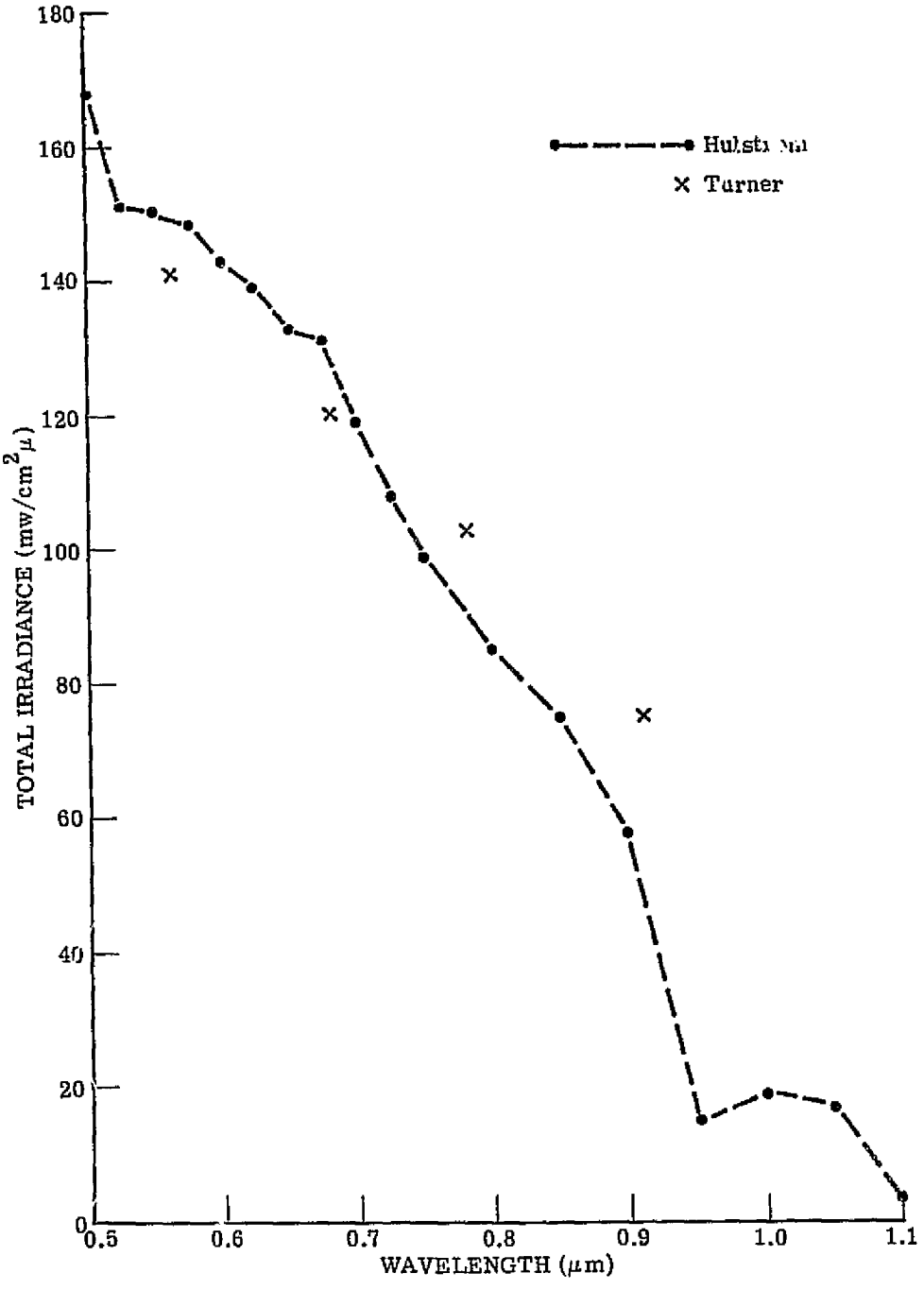

FIGURE 5. COMPARISON OF HULSTROM MEASURED AND TURNER MODEL CALCULATED TOTAL IRRADIANCE FOR GRANITE HILLS SITE, 21 JUNE 1973

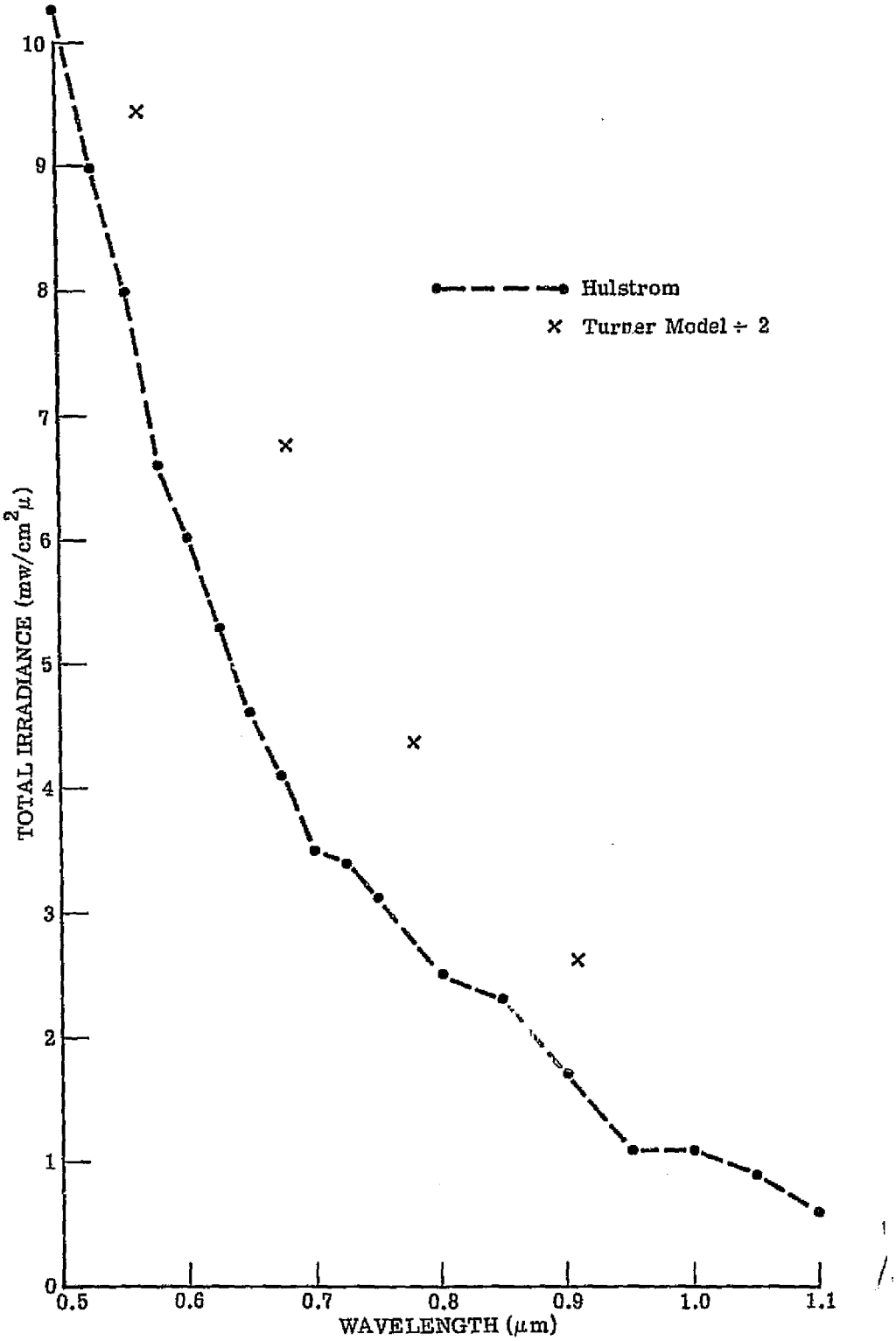

FIGURE 6. COMPARISON OF HULSTROM MEASURED AND TURNER MODEL CALCULATED DIFFUSE IRRADIANCE FOR GRANITE HILLS SITE, 21 JUNE 1973

was calculated by reducing the Rayleigh term by the ratio of pressures at the site and the weather station, and by calculating a new aerosol term assuming an Elterman standard atmosphere. The purpose of such calculations was to bring all measurements to a common base altitude so that horizontal uniformity of the atmosphere could be assessed. (For this comparison, the Cross Creek data were not used since they were taken at a later time than the Granite Hills data.) Table 20 shows the results.

As can be seen from Table 20, the optical thickness computed from the weather records is in all cases, larger than the actual Hulstrom measured value. This may have occurred for three reasons. First, the observers may have underestimated the actual atmospheric visibility in each case, selecting the furthest landmark from the airport and recording its distance as the visibility. Second, there may have been errors introduced in extrapolating the airport measured values to the base elevation of the Hulstrom site. An Elterman profile might not have been appropriate for that day. Third, there may have been horizontal atmospheric variations of such a magnitude as to cause this effect.

Analysis of daily weather maps published by the National Weather Service showed the area to be near the core of a large high pressure area centered over northern Wyoming. The test site was enclosed by the 1024 millibar line indicating high uniform pressure over the area. Colorado Springs and Pueblo reported scattered clouds at about 1000 MST while Salida reported clear skies.

Under these conditions, we would intuitively expect fairly uniform atmospheric conditions over the test site. We would not expect the 38% variance in atmospheric optical depth between Salida's and Hulstrom's measurements. The 3.1% and 10.8% variations between Pueblo and Colorado Springs and Hulstrom's measurements may be mostly explained by experimental and weather observer error. The 48 km visibility reported at Salida is so at variance with the rest of the weather reports and with the Hulstrom measurements that some error in estimation of true conditions must have been made.

The meteorological data suggest a horizontally uniform atmosphere on 21 June 1973 over the Cripple Creek test site. When we try to confirm this by converting weather observer measured visual ranges to equivalent optical thickness, and comparing these results with the Hulstrom measured values, the results are not entirely conclusive, probably because of uncertainty in estimating visual ranges.

3.4 SUMMARY AND CONCLUSIONS

The study of atmospheric effect variations with base elevation in the Cripple Creek test site was conducted with three data sets collected under very clear atmospheric conditions. While this may not be the most extreme situation encountered, it is probably typical of this part of the country.

Under these conditions, the major effect of variations in base elevation is to shift the mean values and alter the covariance matrices of signatures. The resultant effects on pattern recognition or classifier performance are to alter the correct classification percentage, especially of high reflectance targets. We demonstrated changes in the recognition accuracy of snow (16 February 1973) and of exposed granodiorite (20 August 1972) as base elevations varied from 7000 to 13,000 feet. Little change was observed in water and forest classification (20 August 1972) apparently because the classifier decision regions for these classes were large enough to accommodate changes in signatures caused by base elevation variations.

The magnitudes of the effects should be evaluated by anyone attempting to recognize high reflectance targets in areas where there are substantial elevation variations. These effects should also be put into perspective with the variations caused by slope and aspect. Signature variations because of slope and aspect occur because the irradiance on the surface of the target changes. Those effects are expected to be most pronounced for high reflectance targets such as snow and granodiorite, but were not studied quantitatively here.

TABLE 20. COMPARISON OF WEATHER STATION AND MEASURED 0.56 μm OPTICAL DEPTH: CRIPPLE CREEK TEST SITE, 21 JUNE 1973

Station	Visibility (km)	Elevation (ft)	Optical Depth*
Granite Hills	-	8240	0.157
Colorado Springs	104		0.174
Salida	48		0.216
Pueblo	144		0.162

*transformed to 8240 ft elevation

4
DIGITAL-COMPUTER-MAPPING APPROACH

Another part of ERIM's effort was to perform a digital-computer-implemented pattern recognition of Cripple Creek test site terrain units, using data from the ERTS-MSS recorded on computer-compatible tape (CCT). In this section, the flow of operations is discussed in detail and key interaction points with Dr. Smedes and Mr. Ranson are identified. Preparation of the classification map and its display are described and an evaluation of its accuracy presented. Some of the work reported in Section 4.3, addressing the evaluation of map accuracy, was performed by Dr. Smedes and Mr. Ranson; the material is included to broaden the results reported in this document.

4.1 DIGITAL-CLASSIFICATION-MAP PREPARATION

The first step in the Cripple Creek mapping project was the preparation of classification maps of various terrain units. The maps were initially stored on digital tape, then printed out by means of either a computer page printer or special "ink squirter" display. Figure 7 shows the flow of operations for the Cripple Creek study. Operations taking place in all but the last two boxes ("concise display" and "accuracy evaluation") are the subject of this subsection. Succeeding subsections cover the display and accuracy analysis.

The first step in the analysis was to convert the ERTS-MSS CCT's into a format compatible with the ERIM software package. At the same time, we edited out some of the data from ERTS frame 1028-17135, collected on 20 August 1972, so that only data from the test site would be converted in subsequent processing. The MSS-5 (red-channel) image from this frame is shown in Figure 2. Some of the more prominent landmarks of the test site, such as Pikes Peak, Cripple Creek and the Arkansas River, are delineated. We determined from a joint comparison of topographic maps and imagery that data from the second and third tapes (of the four-tape set) completely covered the area. Further, to define the area more precisely, we were able to edit out the first 720 and the last 800 lines of the 2340-line ERTS tapes. The data we copied (and in so doing, converted from ERTS to ERIM format) consisted of lines 720 through 1540 of ERTS tapes 2 and 3. (The eastern boundary of the test site fell about halfway across the area covered by tape 3, but that entire tape had to be converted because the format conversion program could not copy portions of ERTS-CCT records.) By concurrent editing of the data copied, we ended up with about one million pixels for analysis, about one-seventh the number comprising an entire ERTS frame.

The next stage in our processing effort was the preparation of digital "graymaps" of the red MSS-5 data. Using the IBM-7094 MAP, we prepared computer-paper displays of the data, using dark symbols to display low data values and light symbols to display high ones. After

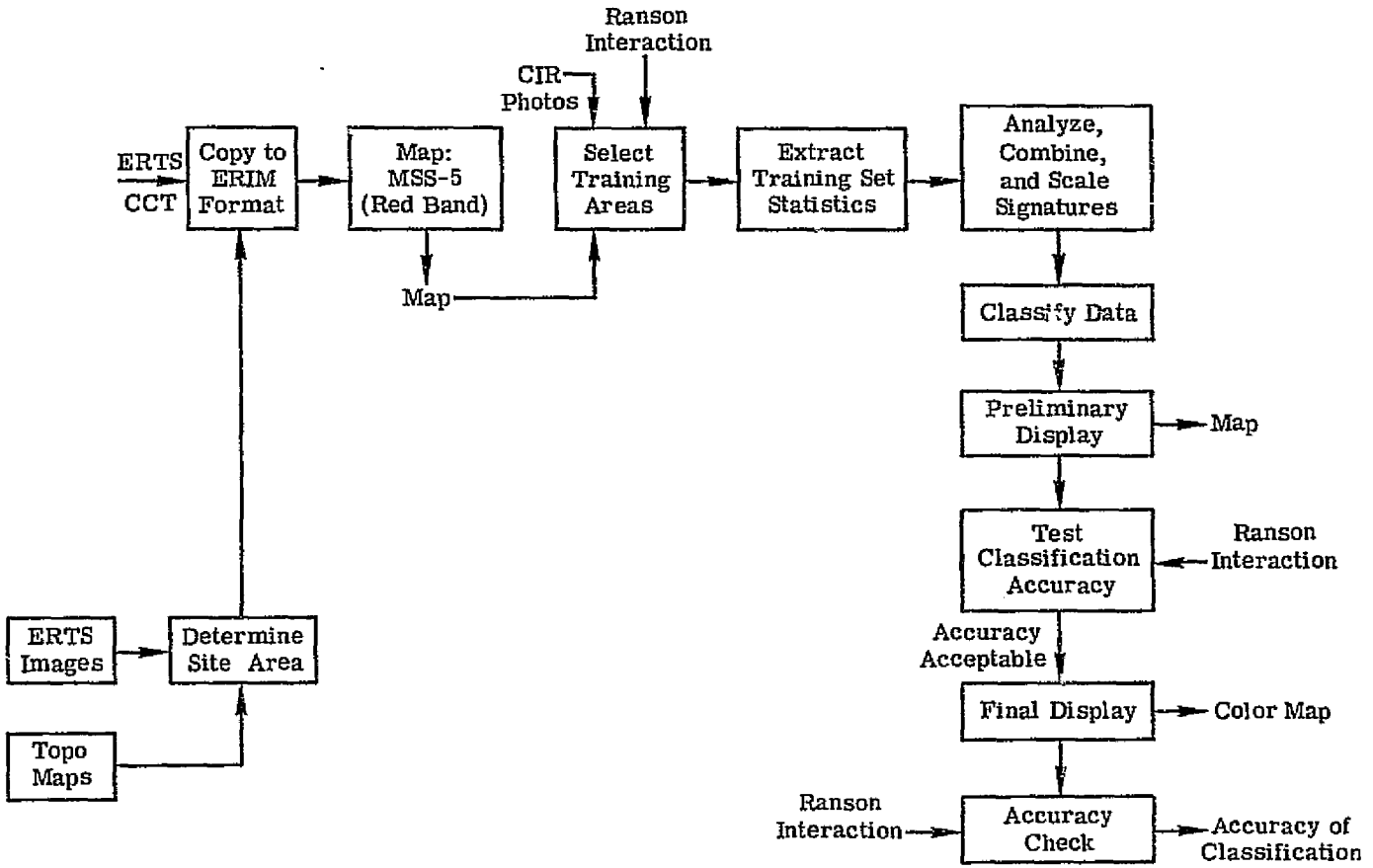

FIGURE 7. FLOW OF DIGITAL-PROCESSING OPERATIONS AND ANALYSIS FOR CRIPPLE CREEK DIGITAL MAPPING PROJECT

several iterations through small portions of the data, we finally obtained a set of symbols and a range of ERTS data values for each symbol that gave a good presentation of the data. Initially, we mapped every other pixel and line of ERTS MSS-5 data, primarily to gain some conception of the material we were working with. This display, when printed on computer paper, was approximately 3 m square and covered nearly an entire wall of one of our workrooms. So, rather than print a map of every ERTS pixel for the whole area, we instead chose and printed small (sample) areas of the data to guide us in our selection of training sets.

The maps generated above were mailed to Jon Ranson at Colorado State University (CSU), Fort Collins for a first attempt at selecting training set areas. He had been analyzing 1:120,000 scale RB-57 color infrared (CIR) and other photography, and had conducted extensive ground investigations within the Cripple Creek test site in an attempt to define training sets for the terrain units to be mapped. Working without benefit of a zoom-transfer scope or other means of registering the digital map (at a scale of about 1:50,000) and the photography, he tried to transfer training set locations from the photography to the digital map. He then sent us line and pixel numbers for several training set areas for each class.

With the line and pixel information supplied by Mr. Ranson, we extracted the spectral signature for each area using the IBM 7094 computer program STAT. The spectral signature is a statistical multivariate quantity, consisting of a set of means (or mean vector), one for each spectral channel, and a covariance matrix. For the area defined, the means represent the average signal level in each band, while the covariance matrix defines the variation in signal in each channel (diagonal terms) and shows how one channel's signal variations are related to those in other channels (off-diagonal terms). Spectral signatures were extracted for all areas identified by Mr. Ranson. The program calculated the statistics and punched a card deck with the signature name, means and covariances; it also printed histograms of the data values in each channel. Editing criteria imposed on the raw data values assured that if they lay so far from the means of the first 200 points as to make it unlikely that they came from the distribution (a χ^2 test at the 0.0001 level is used), they would not be included in the calculation of the signature.

At this point in the analysis, we had just completed a reassessment of the location of the Yellowstone National Park signatures in cooperation with Mr. Ralph Root, another Colorado State University student [7]. Because of the success of training set location technique using color infrared photography enlarged on a VARISCAN viewer to nearly digital graymap scale, we recommended this approach to Dr. Smedes and Mr. Ranson. Mr. Ranson visited ERIM and worked with Mr. Sadowski to revise training set locations and to define final signature classes.

After extracting new spectral signatures from the relocated training sets, we found that 21 classes of materials, as enumerated in Table 21, stood a good chance of being discriminated.

Signatures of different samples of each of the 21 classes were combined to produce spectral signatures that were more representative. Table 21 shows the mean values and standard deviations (in units of digital signal counts) for the 21 signatures used in the preparation of the map for each of the four ERTS bands. We then prepared a new recognition map using the 21 classes and all four ERTS channels. From a preliminary map of the data we became convinced that certain of the classes could not, in fact, be reliably discriminated. Consequently, the recognitions of these terrain units were combined yielding a 13-class final map.

Classification was performed using a modified maximum-likelihood ratio classification algorithm implemented on the IBM 7094 computer. Technical details of this algorithm have been discussed by Crane and Richardson [8]. Classification of the one million pixels, using twenty signatures and all four ERTS bands, took about 25 minutes of 7094 computer time. All of the four ERTS channels were used for classification because previous experience with aircraft multispectral data had shown us that reducing the number of channels below four would significantly degrade the probability of correct classification.

Initially, the classified data were stored in ERIM format on digital tape. Drawing from this data, we prepared preliminary maps of selected areas in order to qualitatively assess classification accuracy in areas of particularly good ground information. For these preliminary maps, all twenty recognition classes were displayed by using as many different symbols to form black and white graymaps. Both Mr. Ranson and Mr. Sadowski analyzed the preliminary maps to determine whether the classes which, from analysis of the signatures, appeared separable would in fact be separable throughout the test site. We found that several classes could not be reliably discriminated.

After consulting with Messrs. Ranson and Sadowski, we decided to display the thirteen classes shown in Table 22.

4.2 DISPLAY OF FINAL RECOGNITION RESULTS

Rather than prepare graymaps of every pixel of the final recognition product, we sought a more concise display. The typical graymap of ERTS data has a scale of about 1:22,000, which would have meant a map of the Cripple Creek test site which was about 3 m square. Such a map is too large to be of practical use for the typical regional resource manager. We had had experience with an "ink squirter" display made by Mead Technology Labs, Dayton, Ohio. For this display medium, pixel size can be as small as 0.35 mm square, or may be made larger in multiples of this size. For our display, we chose to make the pixels 0.7 mm square. This resulted in a 0.5 × 0.7 m map for the Cripple Creek test site at a scale of about 1:100,000. Because ERTS pixels are effectively rectangular (57 m along the scan line and 70 m along the orbital track) while display pixels are square, the resultant map appears

TABLE 21. MEANS AND STANDARD DEVIATIONS OF TWENTY-ONE SIGNATURES USED FOR CRIPPLE CREEK RECOGNITION

	MSS Band***			
Class	4	5	6	7
Forest	17.45 (0.86)	12.26 (0.96)	24.28 (2.44)	13.71 (1.64)
Water	16.35 (1.74)	8.93 (1.84)	5.56 (1.27)	1.00 (0.71)
Meadow	22.87 (1.93)	17.80 (3.29)	46.57 (4.36)	29.43 (3.32)
Pierre Shale	45.42 (1.80)	50.53 (1.95)	48.62 (2.52)	21.17 (1.20)
Niobrara Shale	69.13 (3.98)	81.55 (6.23)	78.41 (5.82)	34.09 (2.82)
Fountain Fm.	34.60 (1.24)	41.30 (1.17)	43.08 (1.88)	20.20 (0.89)
Gruss	37.01 (2.56)	48.34 (5.41)	53.43 (5.84)	24.98 (3.01)
Limestone	46.43 (2.63)	56.89 (3.22)	56.44 (3.61)	28.00 (1.78)
Dakota Sandstone	36.74 (1.47)	41.31 (1.45)	42.47 (1.65)	20.19 (0.95)
Cloud Shadow	16.67 (0.98)	11.67 (1.06)	11.04 (1.00)	4.25 (0.80)
Limestone Composite*	43.07 (2.37)	51.70 (3.95)	54.62 (3.12)	26.49 (1.58)
Dakota Composite*	30.90 (1.84)	31.52 (2.61)	37.37 (2.07)	17.64 (1.08)
Fountain Composite*	31.26 (1.11)	39.58 (2.22)	42.76 (1.68)	20.55 (1.14)
Granite Exposed**	26.36 (1.51)	25.00 (2.24)	41.66 (1.40)	22.65 (1.12)
Granite Composite*	20.83 (1.47)	19.05 (1.69)	30.11 (2.89)	16.57 (1.73)
Granodiorite Exposed**	31.03 (1.39)	31.71 (1.62)	40.64 (1.87)	21.01 (1.04)
Granodiorite Composite*	25.62 (1.10)	24.18 (0.78)	35.35 (1.79)	19.39 (0.80)
Volcanics Exposed*	31.18 (1.45)	30.67 (1.58)	37.57 (1.97)	19.34 (1.19)
Volcanics Composite*	22.65 (1.02)	19.93 (1.00)	28.22 (1.65)	15.44 (1.22)
Alpine Composite*	21.76 (1.66)	17.90 (1.82)	35.92 (3.75)	21.27 (2.80)
Phonolite**	24.82 (1.19)	23.71 (1.96)	38.82 (1.55)	21.53 (0.51)

*combined into Intermediate Forest category in display

**combined into Grassland category in display

***mean values in digital counts with standard deviations in parentheses

TABLE 22. THIRTEEN CLASSES OF THE CRIPPLE CREEK TEST SITE RECOGNITION MAP

1. Forest
2. Water
3. Meadow
4. Grassland
5. Intermediate Forest
6. Pierre Shale
7. Niobrara Shale
8. Fountain Formation
9. Gruss
10. Limestone
11. Dakota Sandstone
12. Cloud Shadow
13. Not Classified

stretched along the scan line. This elongation can be alleviated by geometric correction programs employing "nearest neighbor" interpolation, followed by correction of the recognition tapes.

To produce the color display of Figure 8, we first converted the recognition tapes we had prepared from ERTS tapes 2 and 3, from ERIM format to the special 9-track 800-bpi format required by Mead Corporation. At Mead, the data from the two ERTS tapes were merged so that a single ERTS scan line was written as a single record on tape. Further format conversion was then performed, and the 0.5 × 0.7 m display produced.

Figure 8 was obtained by simply photographing the display. The Mead Corporation charges for producing the display of this data set were approximately $380.

4.3 QUANTITATIVE ACCURACY EVALUATION OF THE 13-CLASS CRIPPLE CREEK TEST SITE MAP

A procedure very similar to that used for the Yellowstone National Park Map [7] was used for assessing the accuracy of the Cripple Creek Test Site Map. However, results from only one test site were available to us at the time this report was written. These results, a confusion matrix, are shown in Table 23.

There was no adequate sample of Dakota Sandstone in the test area selected, so the accuracy of recognition could not be assessed. All classes except Pierre Shale, Gruss and Grassland were recognized correctly more than 65% of the time. The most accurately mapped classes were Forest (87.4%), Water (70.6%), Meadow (73.7%) and Niobrara Shale (85.7%). The high classification accuracies for Forest and Water recognition are consistent with the Yellowstone National Park Study [7], where accuracies of 77%, 100% and 96% for Forest, Intermediate Forest and Water were obtained.

Some qualitative comments about the map itself are in order. Clouds and cloud shadows show recognition patterns which are apparent on the map. While the centers of clouds are not classified, the edges are often recognized as Pierre or Niobrara Shale. Similarly, the edges of cloud shadows are correctly recognized, but many cloud shadow areas have centers recognized as water.

The two white lines running across the upper center of the map are bad data lines and the classifier has called them not classified.

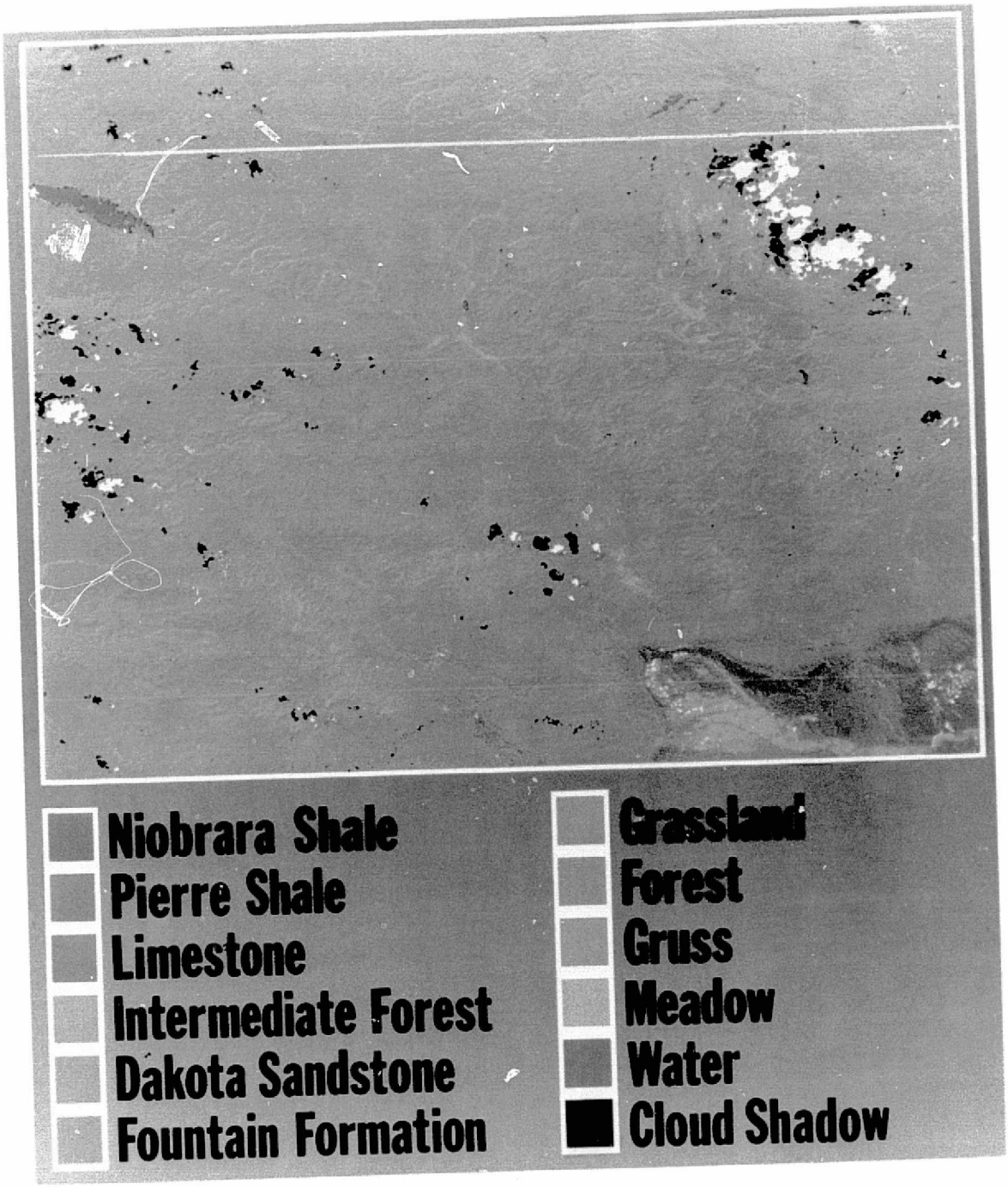

FIGURE 8. COLOR CODED DIGITAL RECOGNITION MAP OF CRIPPLE CREEK TEST AREA PRODUCED FROM ERTS FRAME 1028-17135

TABLE 23. CONFUSION MATRIX FOR ONE TEST SITE OF THE CRIPPLE CREEK TEST AREA

Classifier \ Ground Information	1	2	3	4	5	6	7	8	9	10	11	12
1	87.4	-	-	1.2	7.8	-	3.6	-	-	-	-	-
2	-	70.6	-	-	-	-	-	-	-	-	-	-
3	-	-	73.7	0.7	-	-	-	-	-	-	-	-
4	2.2	-	15.8	71.2	5.7	50.0	-	-	11.1	2.3	-	-
5	9.2	5.9	10.5	19.7	82.6	16.7	3.6	18.5	33.2	20.9	-	-
6	-	-	-	1.8	-	8.3	-	-	11.1	4.7	-	-
7	-	-	-	-	0.3	-	85.7	-	-	-	-	-
8	0.6	-	-	1.8	0.3	8.3	-	67.7	5.6	-	-	-
9	-	-	-	1.2	1.3	-	-	7.7	27.8	4.7	-	-
10	-	-	-	0.6	0.3	-	7.1	-	5.6	65.1	-	-
11	-	-	-	-	0.7	16.7	-	6.1	5.6	2.3	-	-
12	0.6	23.5	-	0.6	0.3	-	-	-	-	-	-	100.0
13	-	-	-	-	-	-	-	-	-	-	-	-
	100.0	100.0	100.0	100.0	100.0	100.0	100.0	100.0	100.0	100.0	-	100.0

Numbers in table are percentages of ground classes (columns) assigned to classifier classes (rows).

See Table 22 for identification of numbered classes.

5
CONCLUSIONS AND RECOMMENDATIONS

We performed pattern recognition classification of terrain classes in the Cripple Creek test site. We also assessed the effects on pattern recognition of variations in atmospheric effects caused by base elevation variations within the test site.

Although we initially tried to recognize more classes, only eleven classes of terrain (with cloud shadow and not classified making a total of 13) could be mapped with acceptable accuracy. All classes except Pierre Shale and Gruss were recognized with greater than 65% accuracy. This assessment was made on only a limited area and may not be representative of the entire area. The accuracy of mapping Dakota Sandstone was not assessed. We found that we could not discriminate sparse forest cover over various substrates. Also the discriminability of some rock units was compromised by sparse grass cover, and these units were combined into a single grasslands category for the final map.

The accuracy of Combined Forest (forest and intermediate forest combined—96.7%) and Water recognition was above 95% for the Cripple Creek test site. This accuracy is very good, and consistent with results obtained in the Yellowstone National Park study previously reported. Because of these accuracies, we feel confident that ERTS data, properly processed, could provide updated green and blue overlays on a 1:250,000 topographic map.

Investigations of atmospheric effects were made on two dates under very clear atmospheric conditions (48 km and 160 km visibilities). Under these conditions the major effect on pattern recognition accuracy seems to be in the accuracy of classifying high reflectance materials. Although variations in path radiance cause changes in the signatures of low reflectance objects, the decision regions for these materials are large enough to accommodate the changes with little if any change in accuracy. By contrast, the classification accuracy of high reflectance objects shows variation with base elevation even at these high atmospheric visibilities. In the investigation of granodiorite recognition, classification accuracy monotonically decreased as base elevation increased. While the mean value of the granodiorite signature did not vary much (because of compensating variations of path radiance and of irradiance and transmission) the covariance matrix terms increased as base elevation increased. Because the volcanics signature closely resembled the granodiorite signature, increased covariance matrix size caused more granodiorite points to be classed as volcanic, thus reducing the correct classification accuracy.

Snow recognition accuracy was shown to vary from 99% at the 9400 ft altitude of the training set to 86% at 8420 ft. This prediction was made theoretically and might not be observed in practice because the snow signature shows saturated values in bands MSS-4, -5, and -6. The predicted snow radiance, when compared with the ERTS-MSS full scale radiance values

would indicate that snow signals should not be clipped for the 16 February date. It is recommended that the saturation of snow signals be examined closely, especially by investigators working on the snow mapping Applications System Verification Test (ASVT).

APPENDIX

CROP SPECIES RECOGNITION AND MENSURATION IN THE SACRAMENTO VALLEY

Frederick J. Thomson

Environmental Research Institute of Michigan
Ann Arbor, Michigan

ABSTRACT

An earlier paper, presented at the 28 September meeting at Goddard, dealt with agricultural recognition maps of a portion of the "San Francisco" frame (1003-18175). The recognition maps were generated by applying multispectral pattern recognition techniques to ERTS-MSS digital taped data. The earlier results have been improved and extended as a result of field studies to check the accuracy of the original recognition. The goal of the second recognition map prepared from these data was to delineate various crop species in a portion of the Sacramento Valley, and at the same time to determine how accurately each could be classified and measured from ERTS-1 data.

The new recognition map, a new and concise display of the old map, and classification and mensuration accuracy data will be presented and discussed. The mensuration accuracy, in particular, is affected by the presence of an edge effect one resolution wide surrounding nearly all fields. Points on the edge are misclassified because they contain a mixture of e.g., crop and bare soil. Using a processing technique to estimate the proportions of unresolved objects in this edge region, a much improved mensuration capability will be demonstrated.

1. INTRODUCTION

Shortly after the launch of the ERTS satellite, the Environmental Research Institute of Michigan (then Willow Run Laboratories of the University of Michigan) obtained digital tapes of the "San Francisco" ERTS frame, designated 1003-18175. The request for these tapes was made so that existing multispectral data analysis software could be tested on ERTS data. To verify the software performance, it was decided to generate a recognition map of a portion of the data. The area selected for analysis was northwest of Sacramento. This 375 sq mi area of intensive, irrigated agriculture was classified into eight categories. The identify of these categories was later verified by ground visits to the site and to Bureau of Reclamation offices.

The initial maps produced were discussed at the Goddard symposium of 29 September 1972 and have been further analyzed by the ERIM staff [9, 10]. While the original maps were good and accurate classifications of the data, two questions remained.

1. It was clear that conventional digital computer page printer displays of ERTS data were cumbersome because of the large quantity of data displayed. While the use of computer page printer data for initial analysis was acceptable, could a more concise display be found for the final classified results?

2. While several economically important crops were classified in the first effort, there were several "salad" categories (categories consisting of several crop species). While this was unavoidable in the first map because of lack of ground information, could a crop species map be generated given training sets for the important crop species in the area?

Because the answers to these questions were felt to be significant to the ERTS data analysis in general, processing of this data set was pursued.

2. CONCISE DISPLAY OF ERTS DATA

ERTS data are delivered in digital tape and film form. For many ERIM analyses, digital tape data are processed for wide area surveys. The concise display of such processed results is clearly important. A conventional page printer display of all the data in one ERTS frame covers a 27 ft × 24 ft area!! While the utility of computer page printer outputs for initial analysis is acceptable, some more concise display of final processed outputs is essential if these processed outputs are to be accepted by users.

Two solutions to the problem exist. First, at ERIM we have good 70 mm filmstrip printers developed for producing aircraft scanner imagery. Through the development of digital to analog (D/A) conversion facilities, we are now able to produce high resolution images of ERTS raw data or processed results on the same printers used for printing aircraft multispectral data. Data from each digital tape of ERTS data may be printed separately and results mosaicked to provide a 9" × 9" display quite comparable to a typical 9" × 9" transparency from Goddard.

Second, we have obtained through the courtesy of Data Corporation, Dayton, Ohio, a color coded recognition map of the Sacramento data presented at the earlier Goddard meeting. This is shown in Figure A-1. This display was produced from digital tape using a special display device developed by Data Corporation. While the cost of the device was too high for us to buy a printer, Data Corporation agreed to make maps at a reasonable price for us. Display sizes up to 40" × 60" are available, and the basic resolution element size is 1/72". The device directs different colored inks at paper to produce an effective color display.

3. CROP SPECIES RECOGNITION AND MENSURATION

After obtaining ground information from the Sacramento Valley area, we were convinced that our first map was an accurate map of agricultural categories in the area. However, we wanted to determine whether the economically important species could be recognized in such an agricultural area. Also we wished to determine how accurately crop acreages could be determined from ERTS data.

First, we attempted to classify the crops of the area, using training sets selected from fields of different crop species as determined from ground information. The results, shown only for the area for which ground information was readily available, are shown in Figure A-2.

We determined that crop species could be discriminated on the basis of signatures. The criterion was the probability of misclassification computed from the signature information. Typical probabilities of misclassification are shown in Table A-1 below. We were unable to discriminate between wheat and barley stubble because the wheat had been harvested and was stubble at the time. Also, tomatoes and sugar beets could not be discriminated, probably because both have dark green foilage and were relatively immature at the time of ERTS coverage.

The probabilities of misclassification are useful for defining separable classes but do not tell the whole story because of the limited training set areas used to calculate these probabilities. So to further test the ability to classify crops, we made a recognition map. (See Figure A-2). The signatures for the recognition map were derived from three fields of each class of vegetation.

FIGURE A-1. CROP SPECIES MAP OF SACRAMENTO VALLEY

FIGURE A-2. CROP SPECIES RECOGNITION MAP FROM SACRAMENTO VALLEY DATA.
ERTS Frame 1003-18175, 26 July 1972.

KEY TO FIGURE A-2 (CROP SPECIES RECOGNITION MAP FROM SACRAMENTO VALLEY DATA) ERTS FRAME 1003-18175, 26 JULY 1972

Color	Class
Green	Rice
Lt. Gray	Safflower
Pink	Corn
Lt. Gray	Milo
Lt. Blue	Alfalfa
Lt. Pink	Stubble
Dr. Blue	Water
Med. Blue	Fallow Field
Red	Bare Soil
Black	Orchard
Lt. Green	Tomatoes
Med. Gray	Melons
White	Not Recogn.

TABLE A-1

SELECTED PROBABILITIES OF MISCLASSIFICATION
FOR SACRAMENTO VALLEY CROP SPECIES

CATEGORIES	PROBABILITY OF MISCLASSIFICATION
Stubble-Wheat*	0.204
Tomatoes-Sugar beets*	0.157
Melons-Sugar beets	0.075
Milo-Sudan	0.059
Tomatoes-Sudan	0.038
Corn-Orchard	0.032
Corn-Milo	0.032
Tomatoes-Melons	0.030

*Combined in Recognition Map

3.1 Analysis of the Recognition Map

We analyzed the recognition map of Figure A-2 to determine the classification accuracy of the various crops on a per field basis.

Rice was well recognized. Of 30 rice fields (other than the training set) examined, all were correctly classified. A field was assumed to be correctly classified if more than 50% of the points (exclusive of the boundary points) were rice. Boundary elements were recognized as corn and occasionally milo.

About half of the dozen safflower fields were correctly recognized. The remainder were called stubble. Examination of the color IR simulated imagery reveals a subtle distinction between the pale yellow tone of safflowers and the white tone of stubble. Apparently, safflowers were mature at the time and some may have been harvested.

Stubble recognition was correct in all 20 areas examined. As previously mentioned, wheat and barley stubble could not be distinguished, and the stubble training set also solidly recognized some safflower fields.

Tomatoes and sugar beets were correctly classified in each of the ten fields examined. There was a tendency for scattered sugar beet and tomato recognition to occur in other areas, particularly in melon fields.

Melons were poorly recognized in the three fields examined. Closer examination of one of these fields on the CIR simulation reveals a varied planting pattern with some areas in melons and some bare areas. Since the recognition map classifies melons in those areas which are planted, and bare soil recognition elsewhere, the map is felt to be more indicative of the true situation than the ground information.

Water was consistently well recognized, with rivers, large irrigation canals, lakes and some flooded fields all recognized. A fallow field signature obtained from one of the flooded fields proved very specific, recognizing that field and one or two others. The combination of the recognition of these two training sets is felt to accurately portray all water in the scene.

Alfalfa, orchard, corn, and milo recognition was disappointing. Areas of these crops were correctly classified, but a great amount of recognition showed up in other areas. Alfalfa and orchard signatures were derived from areas of sparse cover and probably represent only a subtle departure from bare soil. This fact may account for the appearance of so much orchard and alfalfa recognition outside orchards and alfalfa fields.

Bare soil was consistently correctly classified. Sudan grass was also correctly classified in the three areas examined.

3.2 Mensuration

Since we had good success recognizing rice, we addressed the problem of acreage estimation. We had acreages of some fields available from ground information and concentrated on these fields for a test of rice acreage recognition.

At the outset we knew that the boundary elements being misclassified would impair our acreage estimation accuracy. So we estimated the percentage of rice in the boundary elements using special techniques developed by Nalepka [11]. We found that about 75% of a typical boundary element was rice and 25% bare soil and water. This value is in good agreement with the ground measured 50-60 ft irrigation canal width. A canal of this size would occupy about 1/4 of an ERTS digital tape sample point.

The results of acreage estimates for the seven rice fields studied are shown in Table A-2. Notice that all fields are greater than 100 acres in size. Acreage estimates taking only samples recognized as rice are consistently low, even though solid recognition was obtained in each field. Using a revised estimate based on recognition and mixtures, much better acreage estimates are obtained. (Mixtures analysis was used to estimate the amount of rice in the boundary elements. Boundary elements separating two rice fields were assigned equally to both fields.) The improvement in acreage estimation using the mixtures technique is felt to be significant.

TABLE A-2

COMPARISON OF RICE FIELD ACREAGES ESTIMATED BY RECOGNITION AND BY RECOGNITION PLUS CONVEX MIXTURES

RICE FIELD	TRUE ACREAGE	RECOGNITION ESTIMATE	RECOGNITION PLUS CONMIXED
1	150	119	144
2	212	174	205
3	106	71	95
4	159	130	163
5	176	149	179
6	194	173	196
7	224	214	236
TOTAL	1221	1030	1218

4. SIGNIFICANT RESULTS

Several significant results have accrued from this investigation.

1. Concise display of ERTS digital tape video or recognition data can be obtained by D/A conversion of data and printing on 70 mm filmstrip printers developed for the airborne scanner program. Alternatively, special purpose color digital displays may be generated by devices which print in colored inks directly on paper using 0.014" resolution cell size.

2. Accurate crop species recognition can be done in areas of large field agriculture under relatively clear atmospheric conditions. Crops most accurately recognized are those which are green and substantially completely cover the underlying soil. Mature or harvested crops can be discriminated with lesser degrees of accuracy. Crops with incomplete cover can be recognized inside their field boundaries, but recognition also occurs outside agricultural fields yielding a large number of false alarm detections.
3. Accurate acreage estimation of crops in fields 100 acres in size or smaller requires that some estimate be made of the amount of crop contained in possibly misclassified boundary elements. Without this estimate, acreage determined from pattern recognition results will be biased low. The amount of bias increases with decreasing field size, and is also dependent on field shape.

REFERENCES

1. D. Pitts, W. McAllum and A. Dillinger, "The Effects of Atmospheric Water Vapor on Automatic Classification of ERTS Data," in Proceedings of the Ninth Symposium on Remote Sensing of Environment, Environmental Research Institute of Michigan, Ann Arbor, April 1974.

2. J. Potter, R. Hill and M. Shelton, "Effects of Atmospheric Haze and Sun Angle on Automatic Classification of ERTS-1 Data," in Proceedings of the Ninth Symposium on Remote Sensing of Environment, Environmental Research Institute of Michigan, Ann Arbor, April 1974.

3. R. E. Turner and M. M. Spencer, "Atmospheric Model for Correction of Spacecraft Data," in Proceedings of the Eighth Symposium on Remote Sensing of Environment, Environmental Research Institute of Michigan, Ann Arbor, October 1972.

4. _____, ERTS Data User's Handbook, Document No. 71SD4249, NASA, Goddard Space Flight Center, Greenbelt, Maryland, June 1972.

5. R. Hulstrom, "ERTS-1 Atmospheric Data Analysis Summary for February 16, 1973 Overpass," Martin-Marietta Corporation, Denver, Colorado, July 1973.

6. J. R. Muhm, "ERTS-1 Data Analysis," Martin-Marietta Corporation, Denver, Colorado, July 1973.

7. F. Thomson and N. E. G. Roller, "Yellowstone National Park Mapping from ERTS-1 Computer Compatible Tapes," Report No. 193300-50-F, Environmental Research Institute of Michigan, Ann Arbor, September 1974.

8. R. Crane, W. Richardson, R. Hieber and W. Malila, "A Study of Techniques for Processing Multispectral Scanner Data," Report No. 31650-155-T, Environmental Research Institute of Michigan, Ann Arbor, September 1973.

9. F. J. Thomson, M. Gordon and J. Morgenstern, "Environmental Research Institute of Michigan Computer Processing of ERTS-1 MSS Data from the "San Francisco" Frame (1003-18175)," Report No. 011229-4-S, Environmental Research Institute of Michigan, Ann Arbor.

10. F. J. Thomson, M. Gordon, J. Morgenstern and F. Sadowski, "Environmental Research Institute of Michigan Computer Processing of ERTS-1 MSS Data from the "San Francisco" Frame (1003-18175)," Report No. 011229-8-L, Environmental Research Institute of Michigan, Ann Arbor.

11. R. F. Nalepka, H. M. Horwitz and N. S. Thomson "Investigation of Multispectral Sensing of Crops," Technical Report No. 31650-30-T, Willow Run Laboratories, Institute of Science and Technology, The University of Michigan, Ann Arbor, May 1971.